FUNCTION BASED CONTROL FOR MOTION CONTROL SYSTEMS

By
MELTEM ELİTAŞ

Submitted to the Graduate School of Engineering and Natural Sciences
in partial fulfillment of
the requirements for the degree of
Master of Science

SABANCI UNIVERSITY
Spring 2007

FUNCTION BASED CONTROL FOR MOTION CONTROL SYSTEMS

APPROVED BY:

ASIF ŞABANOVİÇ .....
(Dissertation Advisor)

GALİP CANSEVER .....

KEMALETTİN ERBATUR .....

MUSTAFA ÜNEL .....

VOLKAN PATOĞLU .....

DATE OF APPROVAL: .....

FUNCTION BASED CONTROL FOR MOTION CONTROL SYSTEMS

Meltem Elitaş

Electronics Engineering and Computer Science, M.S. Thesis, 2007

Thesis Supervisor: Prof. Dr. Asif ŞABANOVİÇ

Keywords: Motion Control Systems, Function Based Control, Bilateral Control, Parallel Mechanisms

ABSTRACT

Motion control systems are gaining importance as more and more sophisticated developments arise in technology. Technological improvements enhance incorporation of different research areas into the same framework while trying to make systems function in unstructured environments renders the design of control systems increasingly complex.

Since motion systems are complex, they have complex forward or inverse kinematics, or interactions with other systems. In this study, motion of the systems is decomposed into the tasks, so called "functions". Independent controllers are designed for these functions in the function space. It is proven that motion systems will be controlled in the original space if function based control outputs are superposed.

Applicability of this method is demonstrated on bilateral systems and parallel mechanisms. Bilateral systems application proved that function based control can be used in controlling systems with interactions while establishing desired functional relation between them.

Moreover, investigation of a pantograph and a three-legged manipulator, which come from the parallel mechanisms family and have nonlinear and coupled

system dynamics, showed that creating an appropriate reference configuration to realize the task of motion control helps decouple system dynamics.

Satisfactory simulation results show that functional control can be implemented and its characteristics promise successful future designs for motion control systems.

HAREKET KONTROL SİSTEMLERİ İÇİN FONKSİYON TABANLI DENETİM

Meltem Elitaş

Elektronik Mühendisliği ve Bilgisayar Bilimi, Yüksek Lisans Tezi, 2007

Tez Danışmanı: Prof. Dr. Asif ŞABANOVİÇ

Anahtar Kelimeler: Hareket Denetim Sistemleri, Fonksiyon Tabanlı Denetim, Çift Taraflı Denetim, Paralel Mekanizmalar

ÖZET

Hareket denetim sistemlerin önemi teknolojik gelişmelerin artması ile daha da artmaktadır. Teknolojik gelişmeler değişik çalışma alanlarını aynı çatı altında toplamaya teşvik ederken, gitgide karmaşıklaşan yapıdaki denetleyiciler belirsiz yapılı çevrelerde sistemlerin görevlerini gerçekleştirmeye çalışmaktadır.

Hareket denetim sistemleri karışık yapılarından dolayı karışık ileri ya da ters kinematiklere sahip olabileceği gibi diğer sistemler ile karışık etkileşimlere de sahip olabilir. Bu çalışmada, sistemlerin hareketleri "fonksiyon" diye adlandırılan görevlere ayrılmaktadır. Fonksiyon uzayında, bu fonksionlar için bağımsız denetleyiciler tasarlanmaktadır. Sistemin orjinal uzayına geri dönülüp, fonksiyon tabanlı denetleyici çıkışları doğrusal ekleme metodu ile birleştirildiğinde sistemin orjinal uzayında kontrol edildiği ispalanmaktadır.

Bu yöntemin uygulanabilirliği çift taraflı sistemler ve paralel mekanizmalar ile gösterilmektedir. Çift taraflı sistem uygulamaları, bu yöntemin sistemlerin etkileşimini kontrol etmede ve sistemler arasında istenen fonksiyonel ilişkiyi kurabilmede kullanılacağını kanıtlamaktadır.

Ayrıca, bağlı (coupled) ve doğrusal olmayan sistem dinamiklerine sahip olan paralel mekanizmalar ailesinden beş çubuklu bağlam (pantograph) ve üç bacaklı mekanizma incelemeleri, hareket denetim görevlerini gerçekleştirmek için oluşturulan

uygun bir referans yapılandırmanın, sistem dinamiklerini ayırmayı ve basit denetleyiciler elde etmeyi sağladığını göstermektedir.

Deney ve simülasyon sonuçları fonksiyonel denetimin haraket kontrol sistemlerinde uygulanabileceğini ve özelliklerinin bu sistemler için başarılı gelecek tasarımlar vaat ettiğini ortaya koymaktadır.

"To my family"

ACKNOWLEDGEMENTS

I would like to express my sincere appreciations to my advisor Prof. Asıf Šabanoviç for his endless support and advice. I have felt his help and guidance at every step of my life during my master.

Special thanks to Dr. Mustafa Unel and Dr. Volkan Patoglu for long discussions we had about my research and my education. I also thank the rest of my jury members Prof. Galip Cansever, Dr. Kemalettin Erbatur.

I would like to thank all my friends and colleagues: Yesim Humay Esin, Berk Calli, Erdem Ozturk, Selim Yannier, Yasser El Kahlout, Orkun Karabasoglu, Ramazan Unal, Hakan Bilen, Muhammet Ali Hocaoglu, Altug Solak, Ahmet Fatih Tabak, Caner Akcan, Erol Ozgur, Asanterabi Kighoma Malima, Nusrettin Gulec, Utku Seven, Burak Yilmaz, Bahadir Beyazay, Ahmet Ozcan Nergiz, Ozan Mutlu, Yigit Okan, especially, Merve Acer, Erhan Demirok, Elif Hocaoglu, Ertugrul Cetinsoy, Shahzad Khan, Emrah Deniz Kunt, Ahmet Teoman Naskali for their friendship and assistance.

I would also like thank my roommate Emel Yesil, mathematicians Esen Aksoy and Alp Bassa, Kazim Cakir, Mrs. Nadira Šabanoviç, Ilker Sevgen and Dr. Toshiaki Tsuji for their support.

I really believe that meeting with these people at Sabanci University was a big chance for me.

Last but not least, I would like to express my thanks to my parents Gultekin-Mehmet Elitas, my brother Rasit Elitas and my grandparents. They have always encouraged and helped me to pursue my dreams.

This research have been accomplished with the generous financial support from Mr. Yousef Jameel and TUBITAK.

TABLE OF CONTENTS

LIST OF FIGURES

TABLE OF SYMBOLS

q	Vector of generalized positions
q_e	Vector of obstacle positions
$\dot{q}$	Vector of generalized velocities
$\ddot{q}$	Vector of generalized accelerations
$M(q)$	Inertia matrix
$L(q,\dot{q})$	Vector presenting Coriolis and Centrifugal forces
$H(q,\dot{q})$	Vector presenting gravity and friction forces
$N(q,\dot{q})$	Vector of coupling forces including gravity and friction
F	Vector of generalized input forces
F_{ext}	Vector of external forces
m	Second order system inertia matrix
n	Vector of coupling forces for second order systems
Z_e	Environment impedance
Z_h	Human impedance
C_h	Spring coefficient of human
C_e	Spring coefficient of environment
D_h	Damping coefficient of human
D_e	Damping coefficient of environment
$\xi(q,\dot{q})$	Configuration of mechanical system
S_q	Sliding mode manifold for position control
S_F	Sliding mode manifold for force control
$\sigma(\xi^{ref},\xi)$	Control requirement
v	Lyapunov function candidate
D	Positive definite matrix

$\vartheta(\Delta F_e)$	Interaction control input
$g_{ij}(q, q_e)$	The interaction force between system and environment
F_d	Disturbance
$\varsigma_i(q)$	Smooth linearly independent functions of motion
ϕ	System role vector, $\phi \in R^{nx1}$
x_m	Position of master manipulator
x_s	Position of slave manipulator
ε_{x+}	Common mode function of positions
ε_{x-}	Difference mode function of positions
ε_{F+}	Common mode function of forces
T	Transformation matrix
F_h	Master generated force
F_e	Slave generated force
F_m	Generated force for master manipulator
F_s	Generated force for slave manipulator
F_{md}	Disturbance force for master manipulator
F_{sd}	Disturbance force for slave manipulator
ε	Infinity small distance
K_p	Proportional term of PID controller
K_I	Integrator term of PID controller
K_d	Derivative term of PID controller
x_m^{ref}	Position reference for master manipulator
x_s^{ref}	Position reference for slave manipulator
$\dot{x}_m$	Velocity of master manipulator
$\dot{x}_s$	Velocity of slave manipulator
$\ddot{x}_m$	Acceleration of master manipulator
$\ddot{x}_s$	Acceleration of slave manipulator
i_s	Current input for slave

i_m	Current input for master
i_h	Human generated current input for master
V_h	Velocity of human
V_e	Velocity of environment
F_x	Force input for position control
F_F	Force input for force control
K_{FM}	Force coefficient of master motor
K_{FS}	Force coefficient of slave motor
θ_i	Joint angles of pantograph
a_i	Link lengths of pantograph
X_{fi}	Pantograph variables in function space
X_{ri}	Pantograph variables in robot space
ε	Translation function of three-legged mechanism
ε_{ij}	Rotation function of three-legged mechanism
F_{dis_i}	Disturbance force acting on three-legged mechanism
u_i	Control input for three-legged mechanism
S_{ε_i}	Sliding mode manifold for three-legged mechanism
K_u	Sliding mode parameter
D	Sliding mode parameter
C	Sliding mode parameter

TABLE OF ABBREVIATIONS

DOB	Disturbance Observer
RFOB	Reaction Force Observer
SMC	Sliding Mode Control
dof	Degrees of Freedom

1 INTRODUCTION

Modern motion control systems are acting as “agents” between skilled human operator and environment (surgery, microparts handling, teleoperation, etc.). In such situations design of control should encompass wide range of very demanding tasks. At the lower level one should consider tasks of controlling individual systems - like single DOF (degrees of freedom) systems, motor control, robotic manipulators or mobile robots. On the system level control of multilateral interaction between systems of the same or different nature, the remote control in master-slave systems, haptics, parallel mechanisms etc. should be considered. In general design of motion control system should take into account (i) unconstrained motion - performed without interaction with environment or other systems - like trajectory tracking, (ii) motion in which system should maintain its trajectory despite of the interaction with other systems - disturbance rejection tasks, (iii) constrained motion where system should modify its behavior due to interaction with environment or another system or should maintain specified interconnection - virtual or real - with other systems and (iv) in remote operation control systems should be able to reflect the sensation of unknown environment to the human operator.

The possibility to enforce certain functional relations between coordinates of one or more motion systems represent a basis of function based control algorithm. It is demonstrated that motion control problems can be solved while defining motion by tasks which helps to decouple the nonlinear dynamics and makes overall controller design simple.

Decentralized control as a family of function based control system seems a promising framework for applications in motion control systems with concepts such as subsumption architecture [1], multi-agent system [2], cell structure [3], fault tolerant systems [4], and decomposition block control [5]. Under the condition of number of degrees of freedom of each finger is specified for satisfying a condition of stationary resolution of controlled position state variables, overall control input can be designed by linear superposition is shown by Arimoto and Nguyen [6]. Tatani and Nakamura

proposed a method, polynomial design of the nonlinear dynamics for the brain like information processing of whole body motion based on the singular value decomposition [7]. Furthermore, Tsuji, Nishi and Ohnishi developed function based controller design [8]. Onal and Sabanovic implemented a bilateral control using sliding mode control applying functionality [9].

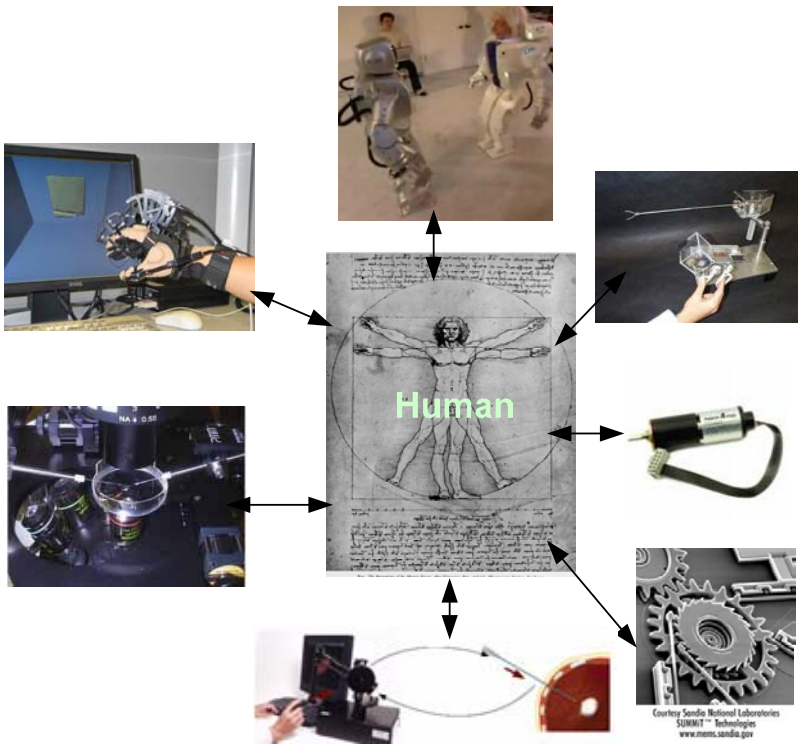

Figure 1-1– Motion control systems

In this study, function based control design is proposed to control motion systems like (iii) and (iv), which considers bilateral control systems and parallel mechanisms as examples. The challenges of these research fields are as follows.

Bilateral systems have functional relations to maintain interactions between master, slave, human and environment while parallel mechanisms have nonlinear and coupled system dynamics.

In literature numerous control algorithms are developed for both bilateral systems and parallel mechanisms. Some methods to obtain stability and total transparency, conformity of force feeling with the real forces, which means of bilateral systems are presented as follows:

Lawrences' papers [10] [11] provide tools quantifying teleoperation system performance and stability when communication delays are presented. It is also shown that transparency and robust stability (passivity) are conflicting objectives, and a trade-off must be made in practical applications. The key to achieving the high levels of transparency is described. H. Zaad has showed the advantages of employing local force feedback for enhanced stability and performance in teleoperation systems [12]. In the presence of time-delays neither transparency nor stability is preserved and new control strategies have to be devised to resolve the problem, however, Katsura proved that whether or not there is time delay in the system, ideal transparency cannot be obtained [13]. Yokokohji and Yoshikawa discuss the analysis and design of master-slave teleoperation systems in order to build a superior master-slave system that can provide good maneuverability [14]. As a result, their control schemes for master-slave manipulators, has been proposed to realize the ideal responses, which can be examined in [15]. In our study, bilateral control is achieved on the intersection of the position and force tracking manifolds. Time delays are not considered.

The study begins in section II with mathematical formulations of control and motion of systems and its extension to general systems in interactions. The following section considers application of function based control architectures to motion control systems. Bilateral control systems are examined in section IV, in order to understand the effectiveness of this method on the systems with coupled dynamics, pantograph and three – legged parallel robot are investigated in section V. Finally, section VI concludes the study.

2 PROBLEM FORMULATION

The goal of this study can be stated as follows: Implement some transformation and obtain basic tasks whose combination realize operator's requirement while having simple controllers and conserving stability of the system.

2.1 Formulations of Mechanical Systems and Interaction Forces

For fully actuated mechanical systems (number of actuators equal to the number of the primary masses) mathematical model may be found in the following form [16], [17]:

$$\begin{aligned} &M(q)\ddot{q} + N(q,\dot{q}) = F - F_{ext}, \text{ where} \\ &N(q,\dot{q}) = L(q,\dot{q})\dot{q} + H\left(q,\dot{q}\right) \end{aligned} \tag{1}$$

$q \in \Re^n$ stands for vector of generalized positions, $\dot{q} \in \Re^n$ stands for vector of generalized velocities, $M(q) \in \Re^{nxn}$, $M^- \le \|M(q)\| \le M^+$ is generalized positive definite inertia matrix with bounded parameters, $N(q,\dot{q}) \in \Re^{nx1}$ $\|N(q,\dot{q})\| \le N^+$ represent vector of coupling forces including gravity and friction, $F \in \Re^{nx1}$, $\|F\| \le F^+$ stands for vector of generalized input forces, $F_{ext} \in \Re^{nx1}$, $\|F_{ext}\| \le F_{0ext}$ stands for vector of external forces. M^-, M^+, N^+ and F^+ F_{0ext} are known scalars. The model (1) may be rewritten as *n* second order systems of the form

$$m_{ii}\ddot{q}_i + n_i = F_i - F_{exti} - \sum_{i=1, j\neq i}^{n} m_{ij}\ddot{q}_j, \quad i = 1,...,n \tag{2}$$

Where elements of inertia matrix are bounded $m_{ij}^- \le \left|m_{ij}(t)\right| \le m_{ij}^+$, functions $n_i^- \le \left|n_i(t)\right| \le n_i^+$ are bounded, elements of the external force vector are bounded by $F_{0i}^- \le \left|F_{exti}(t)\right| \le F_{0i}^+$, and generalized input forces are bounded $F_i^- \le \left|F_i\left(t\right)\right| \le F_i^+$.

External force is a result of system's interaction with environment and in general can be represented by (3) and illustrated in Figure 2-1.

$$F_{ext}(q,q_e) = \begin{cases} F_{ext}(q,q_e) & \text{if there is interaction} \\ 0 & \text{if there is not interaction} \end{cases} \tag{3}$$

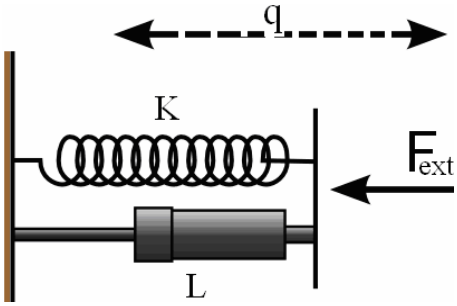

Figure 2-1 – Interation force model

In many cases interaction of the systems is modeled as spring (K) – damper (L), so the interaction force is represented as linear combination of positions and velocities in the following form:

$$F_{ext} = K(q - q_e) + L(\dot{q} - \dot{q}_e) \tag{4}$$

Equation (4) can be applied for modeling virtual or real interactions between systems in s- domain as follows:

$$F_{ext} = Z_e x \tag{5}$$

$$F_{ext} = (K + Ls)x \tag{6}$$

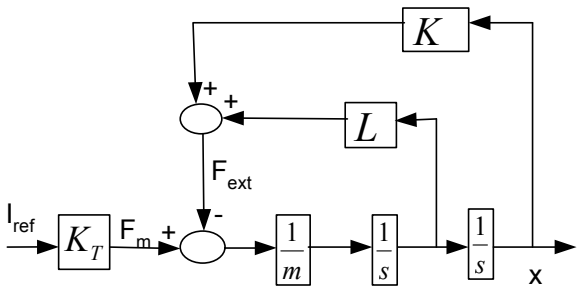

Figure 2-2– Interaction force block diagram

[29] is used to model human and environment with the parameters defined in Table 2-1. In this study, it is assumed that constant spring and damper parameters are used to model human and environment.

Parameters	Descriptions
C_h	Spring coefficient of human
D_h	Damping coefficient of human
C_e	Spring coefficient of environment
D_e	Damping coefficient of environment

Table 2-1 – Parameters used for modeling human and environment

2.2 Control Problem Formulation

Vector of generalized positions and generalized velocities defines configuration $\xi(q,\dot{q})$ of mechanical systems. The control tasks for the motion control systems (1) are usually formulated as a selection of the generalized input such that: (i) system executes desired motion specified as position tracking, (ii) system exerts a defined force while in the contact with environment and (iii) system reacts as a desired impedance on the external force input or in contact with environment. The task (i) requires tracking of the reference trajectory with or without interaction with environment – thus requiring very high stiffness and good disturbance rejection. The tasks (ii) and (iii) are specified for a system being in interaction with environment and both require modification of the system state in order to achieve desired behavior while in the contact. In literature these problems are generally treated separately [8] [10] and motion that requires transition from one to another task are treated in the framework of hybrid control [9]. The most general formulation of the fully actuated mechanical systems can be formulated as a task to maintain desired configuration $\xi^{ref}\left(q^{ref},\dot{q}^{ref}\right)$ of the system. Assume that the control system requirements are satisfied if real and desired configurations of mechanical system satisfy an algebraic constraint expressed as

$$\begin{aligned} &\sigma\left(\xi^{ref}\left(q^{ref},\dot{q}^{ref}\right),\ \xi(q,\dot{q}),\right)=0_{nx1} \\ &\sigma=0_{nx1}\Rightarrow\left(\xi=\xi^{ref}\right) \end{aligned} \tag{7}$$

Now the control problem can be formulated as selection of control input so that solution $\sigma\left(\xi,\xi^{ref}\right)=0_{nx1}$ is stable on the trajectories of system (1).

In this study, without loss of generality, it will be assumed that system configuration can be expressed as a linear combination of generalized positions and velocities $\xi\left(q,\dot{q}\right)=Cq+Q\dot{q}$ and consequently $\xi^{ref}=Cq^{ref}+Q\dot{q}^{ref}$. Now control problem can be formulated as a selection of the control so that the state of the system is forced to remain in manifold S_q:

$$\begin{aligned} &S_q=\left\{q,\dot{q}:\sigma\left(\xi\left(q,\dot{q}\right),\ \xi^{ref}\left(q^{ref},\dot{q}^{ref}\right)\right)=\xi\left(q,\dot{q}\right)-\xi^{ref}\left(q^{ref},\dot{q}^{ref}\right)=0\right\},\\ &\sigma,\xi^{ref},\xi\in\Re^{nx1};\ C,Q\in\Re^{n\times n};\ C,Q>0,\\ &\sigma=\left[\sigma_1,\sigma_2,...,\sigma_n\right]^T \end{aligned} \tag{8}$$

Where $\xi^{ref}\left(q,\dot{q}\right)\in\Re^{nx1}$ stands for reference configuration of the system and is assumed to be smooth bounded function with continuous first order time derivatives, matrices $C,Q\in\Re^{n\times n}$ have full rank, $rank\left(C\right)=rank\left(Q\right)=n$. By selecting $C,Q\in\Re^{n\times n}$ as diagonal (8) can be represented by a set of n first order equations as (9).9)

$$\sigma_i=g_i\left(q_i^{ref}-q_i\right)+h_i\left(\dot{q}_i^{ref}-\dot{q}_i\right)=0,\quad i=1,2,..,n \tag{9}$$

2.3 Selection of Control Input

Design of control inputs for system (1) that will enforce the convergence to $\sigma\left(\xi,\xi^{ref}\right)=0_{nx1}$ and that manifold (8) is reached asymptotically or in finite time. The simplest and the most direct method to derive control is to enforce Lyapunov stability conditions for solution $\sigma\left(\xi,\xi^{ref}\right)=0_{nx1}$ on the trajectories of system (1). Lyapunov function candidate may be selected as $v=\frac{1}{2}\sigma^T\sigma$ with first time derivative $\dot{v}=\sigma^T\dot{\sigma}$. v is not explicit function of time. To ensure stability the derivative of Lyapunov function is required to be negative definite so one can require that $\dot{v}=-\sigma^T\psi\left(\sigma\right)<0$. For

$-\sigma^T\psi(\sigma)<0=-\rho v^\delta<0$ with $\rho>0$ and $\frac{1}{2}\le\delta<1$ stability conditions are satisfied and finite time convergence to sliding mode manifold is obtained. From $\dot{v}=\sigma^T\dot{\sigma}=-\sigma^T\psi(\sigma)$ one can derive $\sigma^T\left(\dot{\sigma}+\psi(\sigma)\right)=0$ and consequently control should be selected to satisfy $\dot{\sigma}+\psi(\sigma)\big|_{\sigma\neq 0}=0$. By differentiating (8) and substituting (1) under the assumption that $C,Q\in R^{nxn}$ are constant and $\left(QM^{-1}\right)^{-1}$ exists, from $\left(\dot{\sigma}+\psi(\sigma)\right)\big|_{\sigma\neq 0}=QM^{-1}\left(F-F_{eq}\right)+\psi(\sigma)=0$ one can find control input as in (10).

$$\begin{aligned} F&=F_{eq}-\left(QM^{-1}\right)^{-1}\psi(\sigma)\\ F_{eq}&=\left(F_{ext}+N\right)-\left(QM^{-1}\right)^{-1}\left(C\ddot{q}-\dot{\xi}^{ref}\right)\end{aligned} \tag{10}$$

The F_{eq} is the control input determined from algebraic equation $\dot{\sigma}=0$. This value of the control input will maintain solution $\sigma=0$ for zero initial conditions.

Obviously the structure of control input depends on the selection of $\psi(\sigma)$, which should be determined in such a way so to ensure stability conditions for solution $\sigma=0$ are guarantied and that $\sigma\to 0$. For continuous time systems this function is most often selected to satisfy $-\sigma^T\psi(\sigma)=-\sigma^T D\sigma$ with $D\in R^{nxn}$ being positive definite matrix. Then control has the following form

$$F=F_{eq}-\left(QM^{-1}\right)^{-1}D\sigma \tag{11}$$

2.4 Equation of Motion

Equations of motion for system (1) with control (10) enforcing stable solution (8) can be derived as (12).

$$\begin{aligned} M\ddot{q}+N&=F_{eq}-\left(QM^{-1}\right)^{-1}\psi(\sigma)-F_{ext}\\ M\ddot{q}+N&=\left(F_{ext}+N\right)-\left(QM^{-1}\right)^{-1}\left(C\dot{q}-\dot{\xi}^{ref}\right)-\left(QM^{-1}\right)^{-1}\psi(\sigma)-F_{ext}\\ M\ddot{q}&=\left(QM^{-1}\right)^{-1}\left[\left(\dot{\xi}^{ref}-C\dot{q}\right)-\psi(\sigma)\right]\\ M\ddot{q}^{des}&=M\ddot{q}\end{aligned} \tag{12}$$

Since matrices $Q \in R^{nxn}$ and $M \in R^{nxn}$ are full rank matrices than $\left(QM^{-1}\right)^{-1} = MQ^{-1}$ and (10) can be rewritten as

$$\begin{aligned} \ddot{q}^{des} &= Q^{-1}\left[\left(\xi^{ref} - C\dot{q}\right)\psi(\sigma)\right] \\ \ddot{q} &= \ddot{q}^{des} \end{aligned} \tag{13}$$

Motion (13) of the system (1) under control (10) depends on selection of the manifold (8) (matrices C and Q) and the reference configuration $\xi^{ref} \in R^{nx1}$. Closed loop system realizes an acceleration controller with desired acceleration defined by (14).

$$\frac{d}{dt}Q^{-1}\left[\left(\xi^{ref} - Cq\right) - \int \psi(\sigma)dt\right] \tag{14}$$

For $\psi(\sigma) = D\sigma$ and $\xi^{ref} = Cq^{ref} + Q\dot{q}^{ref}$ motion (13) becomes

$$\begin{aligned} \ddot{q} &= \left[\left(Cq^{ref} + Q\dot{q}^{ref} - C\dot{q}\right) - D\sigma\right] \\ \ddot{q} &= \ddot{q}^{ref} - Q^{-1}\left(C + DQ\right)\left(\dot{q}^{ref} - \dot{q}\right) - Q^{-1}DC\left(q^{ref} - q\right) \\ \dot{\sigma} + D\sigma &= 0 \end{aligned} \tag{15}$$

Motion (15) depend only on the selection of the design parameters (matrices C, Q and D) and if matrix $D \in R^{nxn}$ is selected diagonal and large enough the ε vicinity of the manifold (8) will be reached fast and then motion of the system will mostly determined by predominant pole defined by matrices C and Q and related dynamics $C\Delta q + Q\Delta\dot{q} = \varepsilon$ with $\varepsilon_{t\to\infty} \to 0$ and consequently $\Delta q = q^{ref} - q$ and $\Delta q_{t\to\infty} \to 0$. Motion (15) for $\psi(\sigma) = D\sigma$ can be interpreted as a PD controller with disturbance feed-forward term and $K_D = Q^{-1}\left(C + DQ\right)$ and the proportional term $K_p = Q^{-1}DC$.

If control is selected in such a way that the manifold (8) is reached in finite time and sliding mode motion instead of n poles defined by D will have n poles in origin and the motion will be governed by $C\Delta q + Q\Delta\dot{q} = 0$. $\Delta q = q^{ref} - q$ so that $\Delta q_{t\to\infty} \to 0$ when $t \to \infty$. Equations (15) shows that in ideal case, motion of the system will not be modified when it comes in contact with environment, thus this solution is suitable for solving position-tracking problem of mechanical systems.

2.5 Modification of System Configuration

Changing the reference configuration of the system $\xi^{ref}(q^{ref},\dot{q}^{ref})$ causes the system motion modification. This way definition of control goal and behavior of the system is clearly resting on the selection of the reference configuration and its dependence on desired specifications [16] [17]. Due to the fact that in fully actuated systems interaction forces and system configuration cannot be set independently, hybrid schemes had been developed to cope with position-force control tasks and the transitions from one to another [9]. In the following sections we will concentrate on the selection of the reference configuration for problems of controlling systems required to satisfy certain functional relations (real or virtual).

Assume that the overall external force consists of the disturbance F_d that should be rejected by the system controller including disturbance observer, and the interaction force between system and environment $g_{ij}(q,q_e)$ that should be maintained so that $F_{ext}=F_d+g_{ij}$. As a control task assume the requirement of trajectory tracking and the modification of the system configuration in such a way that the desired interaction between system and environment is maintained. Since trajectory tracking is basic task in mechanical systems it will be natural to assume that function $\xi^{ref}(q^{ref},\dot{q}^{ref})$ depends on the desired trajectory and that the trajectory should be modified the systems in contact with environment in order to maintain desired interaction. For such a behavior of the system (1) the desired manifold (8) should be changed to include the environmental interaction control. In addition, while in contact with the environment motion system is required to modify its trajectory in order to control interaction between system and environment. One possible structure that includes both requirements may be selected as in (16)

$$
\begin{aligned}
&S_{qg}=\left\{q,\dot{q}:\sigma=\xi(q,\dot{q})-\xi^{ref}-\vartheta(\Delta g_{ij})+\Gamma g_{ij}\right\}\\
&S_{qg}=\left\{q,\dot{q}:\sigma=0\right\}\\
&\xi^{ref}(q^{ref},\dot{q}^{ref})=Cq^{ref}+Q\dot{q}^{ref}\\
&\xi(q,\dot{q})=Cq+Q\dot{q}\\
&g_{ij}=\begin{cases}g_{ij}(q,\dot{q},q_e,\dot{q}_e) & \text{with contact}\\ 0 & \text{without contact}\end{cases}
\end{aligned}
\tag{16}
$$

In this study, interaction force with environment is estimated by RFOB.

The interaction control input $\vartheta(\Delta \mathbf{F}_e)$ should be determined to maintain stability of system motion in manifold

$$S_F = \{(q,\dot{q}) : \sigma_F = F(q,\dot{q}) - F^{ref}(t)\}$$
$$S_F = \{(q,\dot{q}) : \sigma_F = 0\} \tag{17}$$

Note that, either motion of the system or the environment can be modified in order to attain desired interaction, and that interaction may be representing a real or virtual force. Motion of systems in interaction is treated here the same way as force control. Actually, not only that the concept is the same but the structure of the controller remains the same. The only difference is in the selection of the interaction term and its measurement or estimation.

3 FUNCTION BASED CONTROL

3.1 Definitions

Complexity of controller design is one of the centre problems for motion control systems in human environment. Human environment has many variables so that robots need a hyper - DOF mechanisms in order to execute multiple actions in parallel. Tsuji, Onhisi and Nishi define the system role and functions in [18]. In this study, system role means motion. The control system should be designed to realize the desired motion. However, it is difficult to associate a motion with a controller directly since it considers different numbers tasks so that the idea of functionality is introduced as minimum components of motion [20] which means tasks of motion. Conversely, motion is described as combination of tasks. This definition composed the bases of this study.

In the situation depicted above motion control systems maintain desired functional relation (for example bilateral control or cooperating robots etc.). In such systems, control should be selected to maintain a functional relation by acting on all of the subsystems.

Assume a set of *n* single dof motion systems each represented by (18)

$$S_i : m_i(q_i)\ddot{q}_i + n_i(q_i, \dot{q}_i, t) = f_i - f_{iext}, \quad i = 1,2,...,n \tag{18}$$

or in the vector form

$$S: \; M(q)\ddot{q} + N(q, \dot{q}, t) = BF - d_{\Sigma} \tag{19}$$

$q \in R^{n\times 1}$, rankB = rankM = n , vectors N, d_{Σ} satisfy matching conditions. Assume also that required role $\Phi \in \Re^{n\times 1}$ of the system S may be represented as a set of smooth linearly independent functions $\zeta_1(q), \zeta_2(q), ..., \zeta_n(q)$ and role vector can be defined as $\Phi^T = \left[\zeta_1(q) \;\; ... \;\; \zeta_n(q)\right]$. Consider problem of designing control for system (18) such that role vector $\Phi \in \Re^{n\times 1}$ tracks its smooth reference $\Phi^{ref} \in \Re^{n\times 1}$.

This part of the study defines function based control framework for constrained motion systems. Let sliding mode manifold $\sigma_{\phi} \in R^{n\times 1}$ be defined as

$$S_{\phi} = \left\{ (q, \dot{q}) : \xi^{ref}{}_{\phi}\left(\phi^{ref}, \dot{\phi}^{ref}\right) - \xi_{\phi}\left(\phi, \dot{\phi}\right) = \sigma_{\phi}, \sigma_{\phi} = 0 \right\} \tag{20}$$

By calculating $\dot{\phi} = \left[\frac{\partial \phi}{\partial q}\right]\dot{q} = J_{\phi}\dot{q}$, one can determine $\ddot{\phi} = \hat{B}F + \hat{d}_{\Sigma}$ where $\hat{B} = J_{\phi}M^{-1}B$ and $\hat{d}_{\Sigma} = J_{\phi}M^{-1}\left(-N(q,\dot{q},t) - d_{\Sigma}\right) + \dot{J}_{\phi}\dot{q}$. By introducing $Q_{\phi} = \left[\frac{\partial \xi_{\phi}}{\partial \dot{\phi}}\right]$ and $C_{\phi} = \left[\frac{\partial \xi_{\phi}}{\partial \phi}\right]$ projection of the system motion on manifold S_{ϕ}, can be expressed as $\frac{d\sigma_{\phi}}{dt} = Q_{\phi}\hat{B}F + \left(\hat{d}_{\Sigma} + C_{\phi}\dot{\phi} - \dot{\xi}_{\phi}^{ref}\right)$. With $\hat{d}_{\phi} = \hat{d}_{\Sigma} + C_{\phi}\dot{\phi} - \dot{\xi}_{\phi}^{ref}$ and $F_{\phi} = Q_{\phi}\hat{B}F$, it can be simplified as $\dot{\sigma}_{\phi i} = F_{\phi i} + \hat{d}_{\phi i}$, $i = 1,...,n$ for which design of control $F_{\phi i}$ is straightforward. If $\left(Q_{\phi}\hat{B}\right)^{-1} = \left(Q_{\phi}J_{\phi}M^{-1}B\right)^{-1}$ exists then inverse transformation $F = \left(Q_{\phi}\hat{B}\right)^{-1}F_{\phi}$ gives control in the original state space. Since $M \in R^{n\times n}$ and $B \in R^{n\times n}$ are

square full rank matrices then one can determine conditions that matrices J_ϕ and Q_ϕ should satisfy in order that $\left(Q_\phi J_\phi M^{-1} B\right)$ exists. Since $Q_\phi, J_\phi, M, B \in R^{nxn}$, sufficient conditions for having unique solutions or control F is $rank\left(Q_\phi J_\phi\right) = n$.

3.2 Structure of Functions

A control system, which interacts with the human environment, is divided into functions and a large hybrid system is composed based on combination of these functions. Controllers have direct relationship with functions while the relationship between functions and robots are complex. They take function-based information from each robot and provide inputs to the robots at the same time as the same as every controller does, but the difference is; individual controllers are directly related to functions instead of control objects and this simplifies controller design in decentralized control systems while composing modular controllers which can be used to execute different tasks. The function based controllers and outline of the coordinate transformation are shown in Figure 3-1.

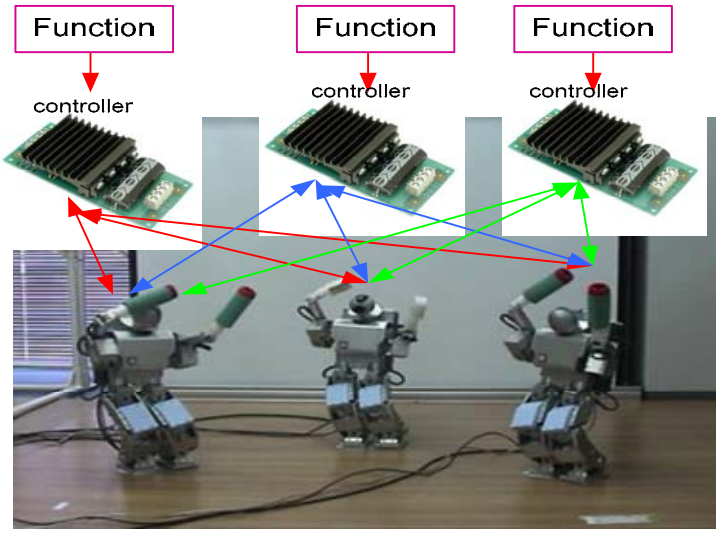

Figure 3-1– Functions, controllers, robots and their Relationships

Functions consider two sub functions one of them is “Task Function” functions of necessary tasks and the other category is “Performance Limit Function” functions of

performance limit like safety, mechanical limits, and workspace boundaries [20]. Performance limit functions become active when exceptions occur.

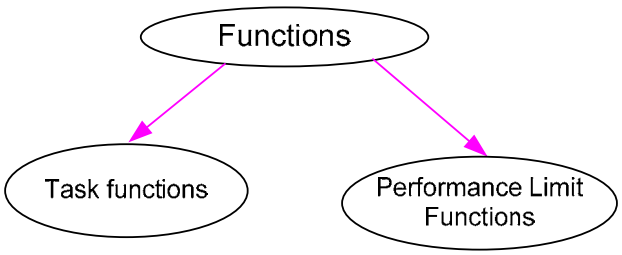

Figure 3-2– Categorization of functions

Functional relations can be represented as Figure 3-2 and Figure 3-3.

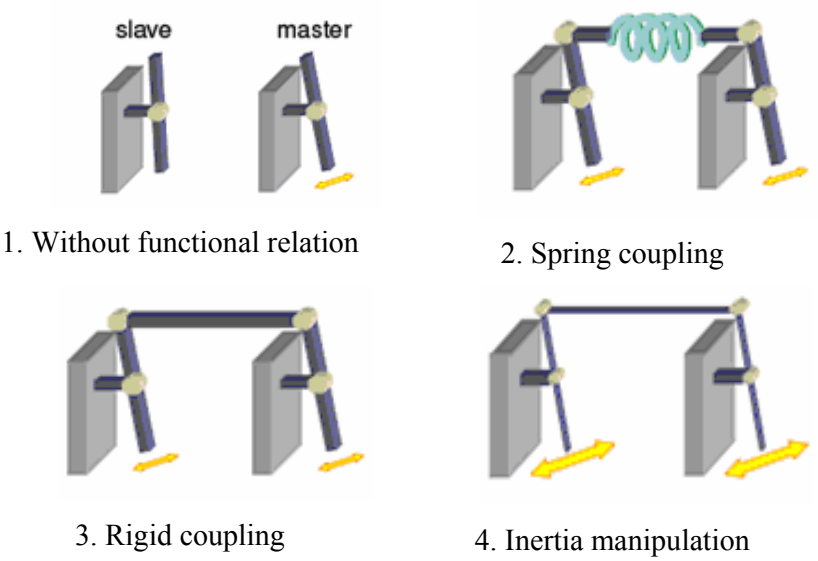

Figure 3-3–Examples of functions [13]

In Figure 3-3, in the first quadrant master and slave robots without any functional relation is shown. In the second one, relation between master and slave robots is spring effect; master and slave arm are connected by a virtual spring, if master arm moves position of slave arm moves to get spring its initial position. In the third one, rigid coupling relation is illustrated, when master moves slave moves in order to preserve the constant distance between them. Finally, the last figure demonstrates inertia manipulation function, which occurs when external forces act. With the assistance of inertia manipulation function, action force on the master can be felt by the slave.

Simulations and experiment will make easy to understand dividing motion into tasks and using functional controllers to control each task, which means realizing desired motion.

3.2.1 Simulation and Experimental Results

3.2.2 System Specifications

The aim of simulation and experiment is to make function based control framework more understandable. Simulation is done to confirm the performance of the proposed controllers, before implementation. Parameters of manipulators and controllers used in the simulation and experiment are the same and represented in Table 3-1.

Figure 3-4–Experimental system [45]

3.2.3 Simulation

Figure 3-5 illustrates simulation diagram of function based controllers including disturbance observers (DOB) and reaction force observers (RFOB) [19]. In this figure, motor_I, motor_II and disturbances F_{md}, F_{sd} are in robot space, while virtual objects, rigid coupling, grasp and inertia manipulation functions are members of function space.

Manipulator parameters	Parametreler
Arm length	0.162 m
Rated motor power output	22.1 W
Rated motor torque output	132 mNm
Number of encoder pulse	512 P/R
Controller parameters (Dspace 1103)	Parameters
Sampling time	0.001 s
Cutoff frequency of DOB	500 Hz
Position gain	P = 15
Velocity gain	D = 0.3
Force gain	K_f =1.5
Motor type	2642 012 CR series graphite commutation DC Micromotor
Gearhead	26/1 series Faulhaber Planetary gearhead with 43:1 gear ratio
Encoder	IE2 – 512 Lines per Revolution Magnetic Encoder

Table 3-1– Manipulator and controller parameters

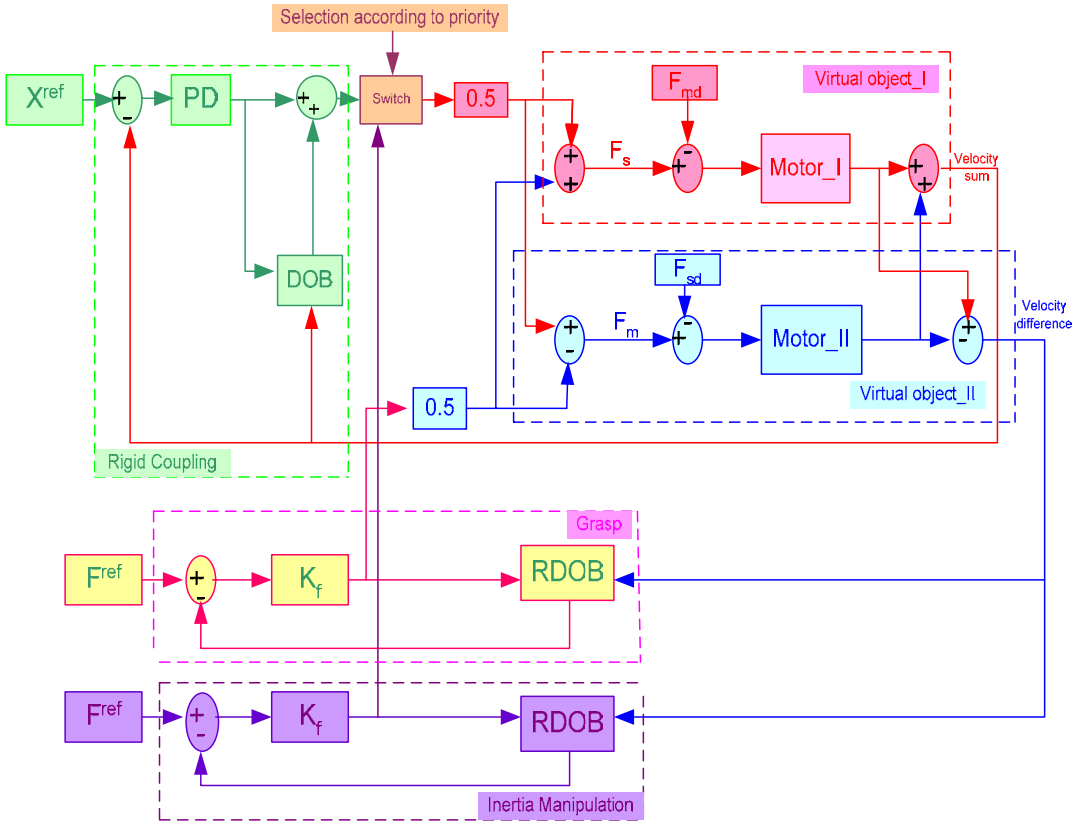

Figure 3-5– Function based control architecture

In this configuration PD controller and proportional controller K_f are used as discussed in section 2.4

For this example rigid coupling functions can be expressed as (21) and (22). (21) corresponds to set the difference between two robot arms zero while (22) sets the values constant.

$$\varepsilon_{x+}(t) = x_m(t) + x_s(t) \tag{21}$$

$$\varepsilon_{x-}(t) = x_m(t) - x_s(t) \tag{22}$$

Model of 1 dof manipulators can be described by $m_i\ddot{x}_i + n_i\left(x_i, \dot{x}_i\right) = F_i - F_{disi}$, $i = 1, 2$ and the virtual plants are calculated as follows:

$$\ddot{\varepsilon}_+ = \frac{1}{m_1}F_1 - \frac{F_{dis1}}{m_1} + \frac{1}{m_2}F_2 - \frac{F_{dis2}}{m_2} \tag{23}$$

$$\ddot{\varepsilon}_- = \frac{1}{m_1}F_1 - \frac{F_{dis1}}{m_1} - F_2 + \frac{F_{dis2}}{m_2} \tag{24}$$

$$u_1 = \frac{F_i}{m_i}, i = 1, 2,\ d_+ = \sum_{i=1}^{2}\frac{F_{disi}}{m_i},\ d_- = \frac{F_{dis1}}{m_1} - \frac{F_{dis2}}{m_2} \tag{25}$$

$$\ddot{\varepsilon}_+ = u_1 + u_2 - d_+ \rightarrow \ddot{\varepsilon}_+ = u_+ - d_+ \tag{26}$$

$$\ddot{\varepsilon}_- = u_1 - u_2 - d_- \rightarrow \ddot{\varepsilon}_- = u_- - d_- \tag{27}$$

After eliminating disturbances by the help of DOB, transformation matrix between virtual objects and control inputs can be obtained as follows:

$$T = \begin{bmatrix} \dot{\varepsilon}_{x+} \\ \dot{\varepsilon}_{x-} \end{bmatrix} = \begin{bmatrix} 1 & 1 \\ 1 & -1 \end{bmatrix} \begin{bmatrix} u_1 \\ u_2 \end{bmatrix} \quad (28)$$

For the first part of simulation, 10 cm position reference is given to ε_{x+}. It is observed that while ε_{x+} traces the reference; there is no control or action on ε_{x-}. Simulation result for function space is shown in Figure 3-6, ε_{x+} realizes its task and reaches steady state very fast. In robot space, motor_I and motor_II reach the half of the command value to realize the system role, as seen in Figure 3-7. As shown in Figure 3-5, rigid coupling function and inertia manipulation function are used in this part of the simulation.

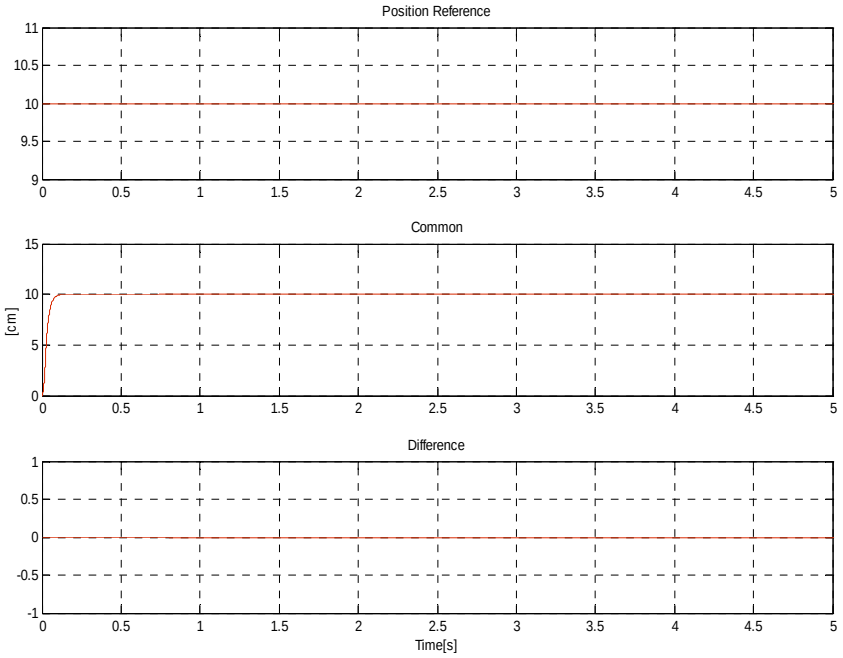

Figure 3-6- Position response to rigid coupling and inertia manipulation functions in function space

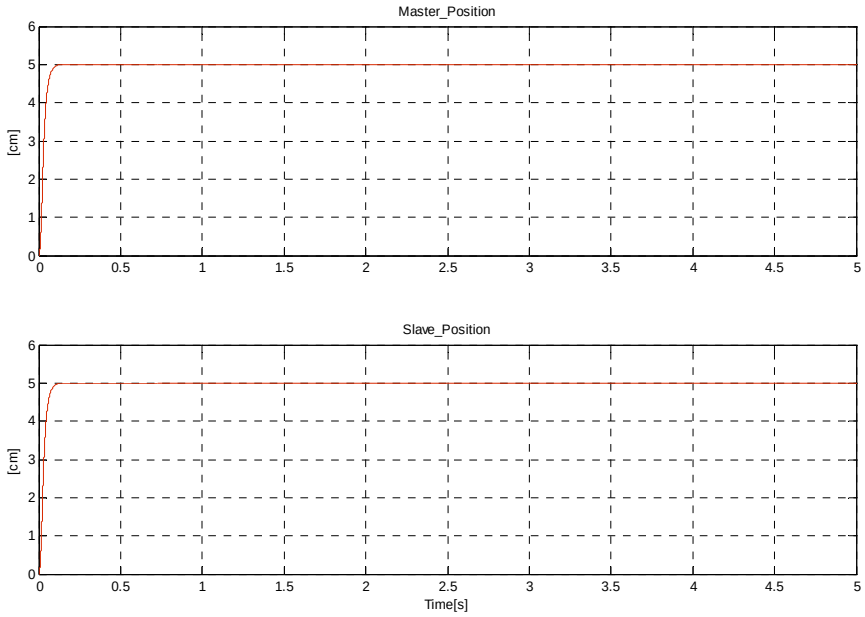

Figure 3-7– Position response to rigid coupling and inertia manipulation functions in robot space

The second part of simulation considers grasp - rigid coupling functions combination. 1.5 N grasping force reference is applied. The simulation result shows the force -1.5 N because forces are considered as action and reaction, Figure 3-8.

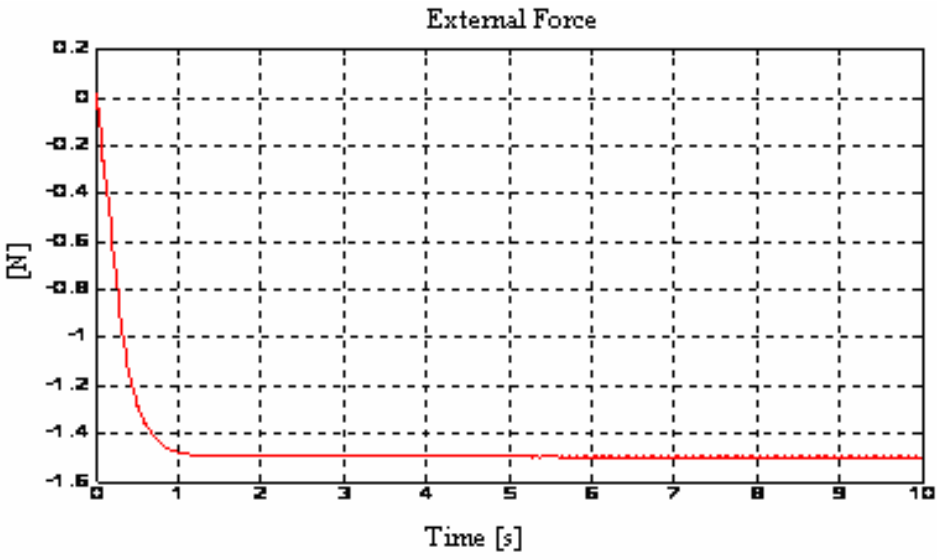

Figure 3-8– Force response to grasp function

Finally, the last part of simulation is an example for grasp – inertia manipulation functions combination. While the load was grasping with 1.5 N forces, it is moved freely by 1.7 N forces. The RFOB outputs are shown in Figure 3-9.

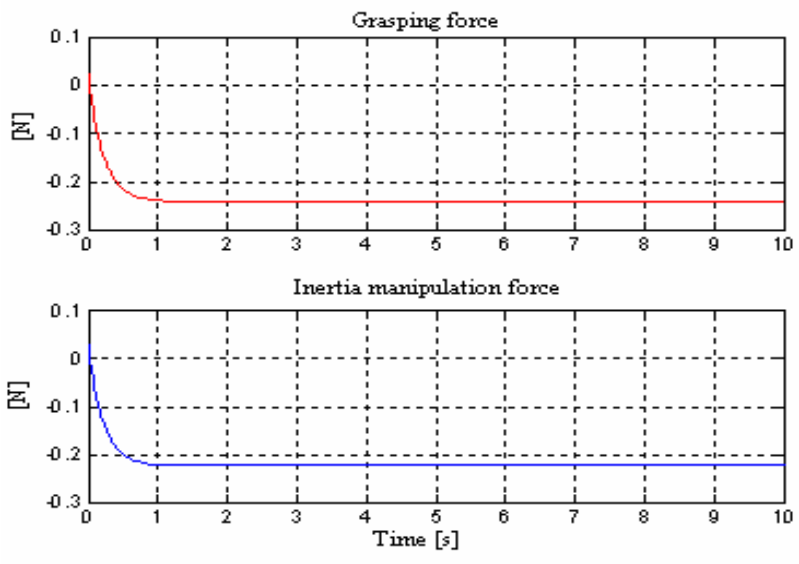

Figure 3-9– Force response to grasp and inertia manipulation functions

Simulation results are satisfactory. Although commenting on some of the results is not very easy for simulation, like moving virtual load freely, experimental results make system more intelligible.

3.2.4 Experiment

After obtaining satisfactory simulation results, an experiment is implemented on the shown set up in Figure 3-4 with the parameters in Table 3-1. The scenario executed in our experiment as follows,

Step_1, the distance between the manipulators is set constant, external force is applied to the manipulators, and they moved through the force while preserving the constant distance.

To execute this scenario a rigid coupling and an inertia manipulation functions are used. Rigid coupling function put the distance between the manipulators constant, we want manipulators to move opposite direction instead of following each other, when an external force is given. The illustration of the experiment is shown in Figure 3-10.

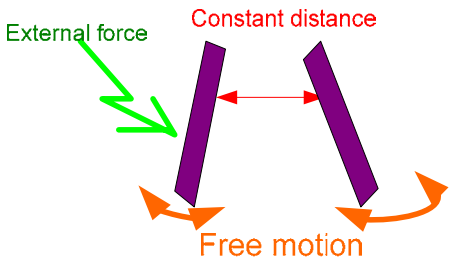

Figure 3-10– Illustration of rigid coupling and inertia manipulation functions

System response is shown on function space in Figure 3-11 and on robot space in Figure 3-12. By the help of external force, system moves, motions of manipulators are completely opposite directions as seen in Figure 3-12. Consequently, sum of their positions are zero in Figure 3-11.

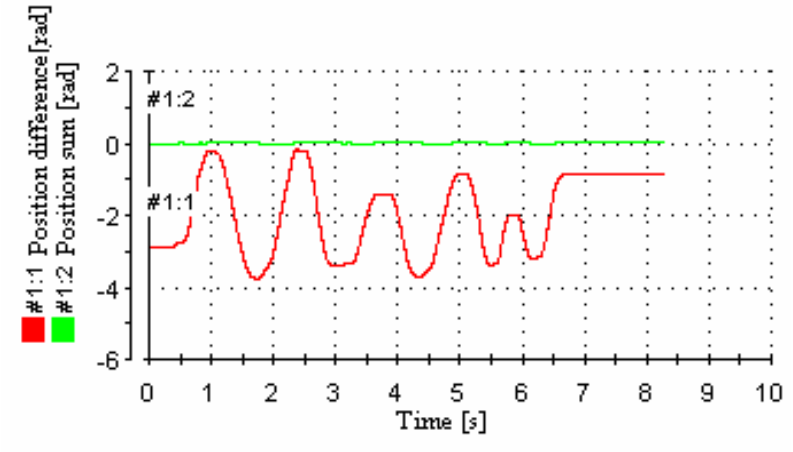

Figure 3-11– Position response to rigid coupling and inertia manipulation functions

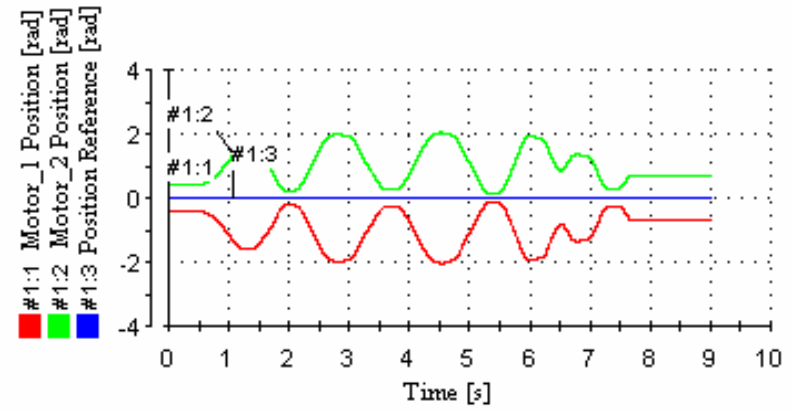

Figure 3-12– Position response of motors to rigid coupling and inertia manipulation

Step_2, the difference is that a load is pinched by hand so the manipulators should grasp it. The priority ordered functions in transformation matrix has changed and instead of inertia manipulation, grasp function is put.

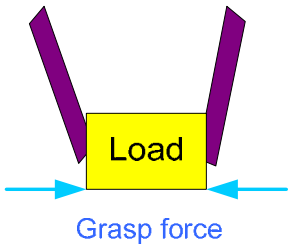

Figure 3-13– Illustration of rigid coupling and grasp functions

As a command grasping force 1.7 Nm is applied.

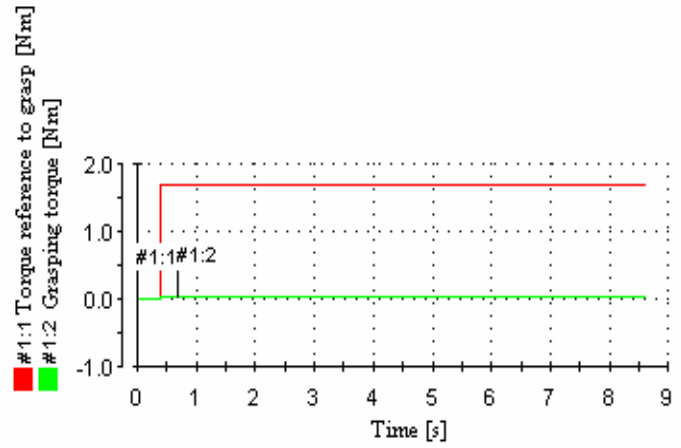

Figure 3-14– Torque response of system to grasp a load

There is no change over of tasks. The hand is taken off from the manipulators at about 0.48 s.

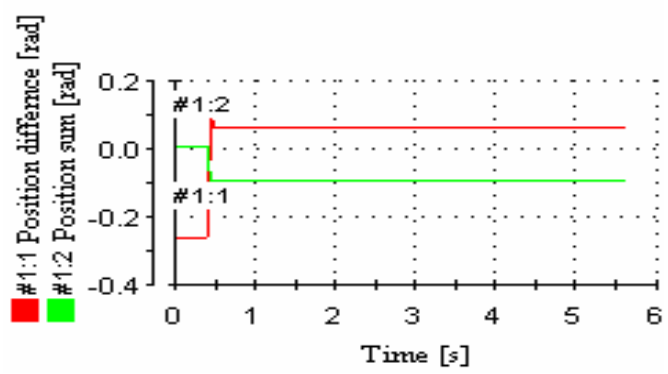

Figure 3-15– Manipulators are carrying a load

Step_3, the aim of this step is to move freely the load while the manipulators grasped it. Inertia manipulation function takes place instead of the rigid coupling function, the illustration is as Figure 3-16.

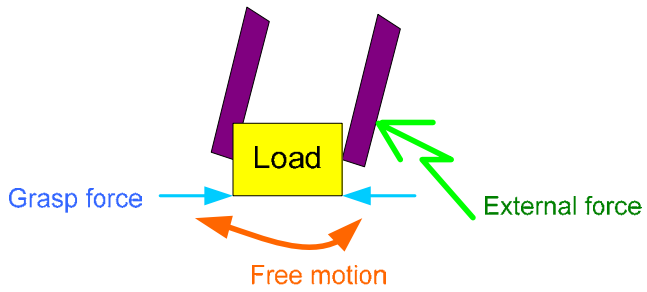

Figure 3-16– Position response to rigid coupling and inertia manipulation functions

Figure 3-17 shows the grasped loads is moving freely by hand.

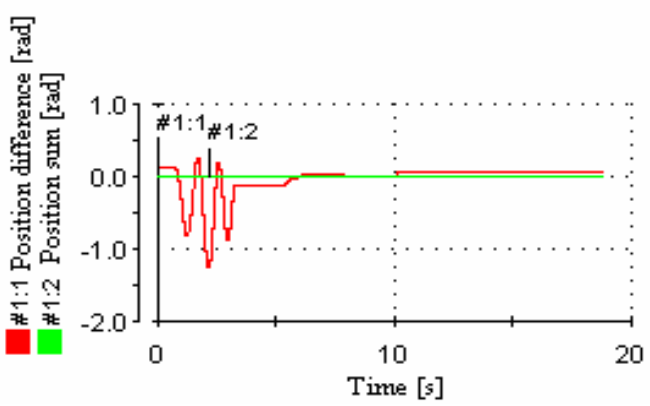

Figure 3-17– The load is moving freely

Finally, the steps executed up to now are made by one after another with respect to time so we can decide whether controller realized the wanted tasks without any problem. The final algorithm and results are as follows [19]:

t < 10: Rigid coupling + inertia manipulation functions are used,

t = 10: Inertia manipulation function → grasp function,

10< t <20: Tasks are the same only the hand was taken off from the manipulators,

t > 20 Rigid coupling function → inertia manipulation function. The load moved freely while it was grasp by the manipulators.

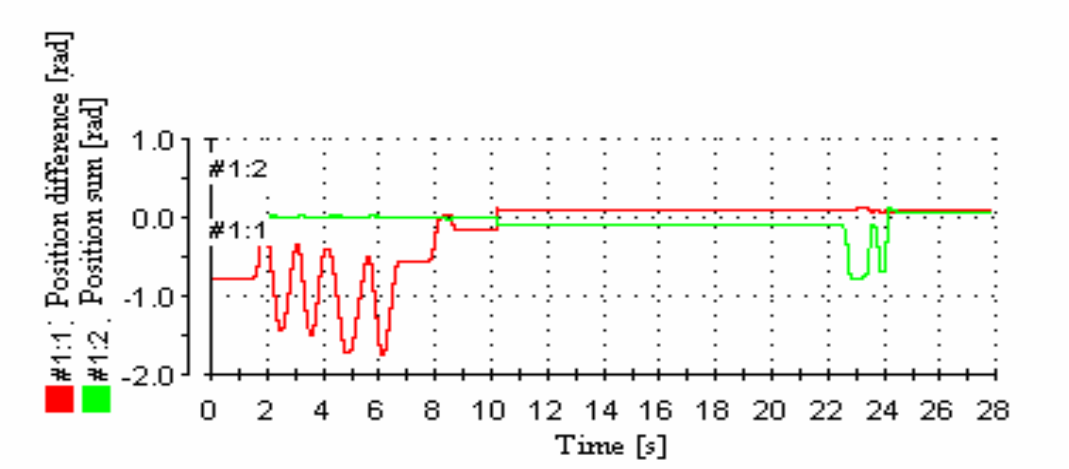

Figure 3-18– Position response with function variations

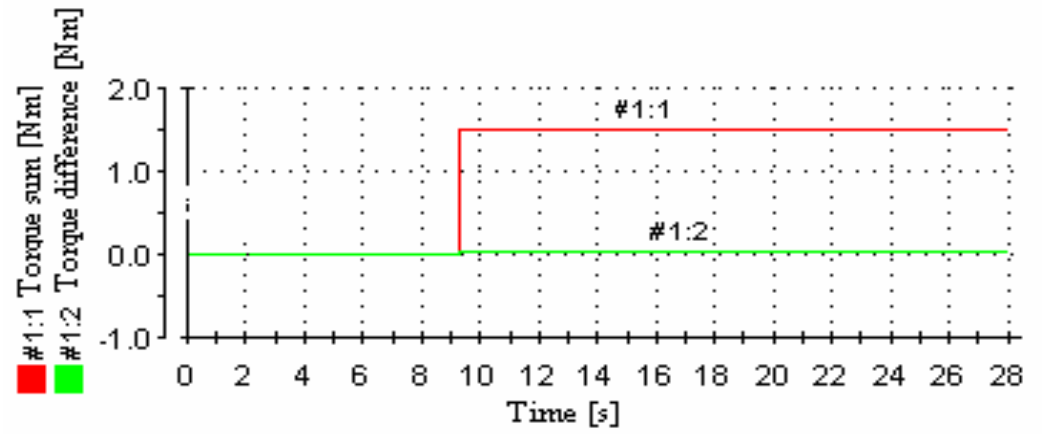

Figure 3-19– Force response with function variations

Figure 3-18 and 3-19 shows the proposed control architecture results to realize desired system motion.

The steps of the motion between 0 to 28 seconds occur according to changes of actions in the environment. While environment is online known, priority of actions in this environment is unknown. Changing priority causes switching of the actions. This experiment is done to understand the functionality so any stability issues about switching is not investigated.

In this chapter, it is shown that functional framework supply systems to be controlled based on tasks. What you want from your system is to realize the desired motion by divided tasks.

4 BILATERAL CONTROL

4.1 Introduction to Bilateral Systems

Researchers have studied bilateral systems for along time, however, in recent decades; the ability that wants from these systems has changed. People want machines not to work only in closed environment according to defined tasks, but also work in open environment where it changes significantly and needs human adaptation. What we called as classical framework is four-channel control architecture and developed by many researchers for along time ago. Function based control framework is intended to generalize the structure of bilateral systems to multilateral systems and make modern motion control systems adaptable to the human environment by maintaining interactions with systems or between systems and environment. Adaptation to the human environment needs good force sensation. If this is achieved using force sensors, force sensors will create some problems about their limited bandwith as well as the force sensed by these sensors has some disturbance from the environment or system, when sensors are added to the system, their dynamics are also added [44]. Functional controllers have their own disturbance observers and force reaction observers [21] in their design so that all plants are nominal and the sensed forces are without disturbance. Functional framework has adaptation to the environment due to its structure. It considers priority ordered functions for changed environment.

In this chapter, the goal is to show advantages of functional framework for bilateral systems. Structure of the chapter is; first a general description of bilateral systems will be given. What are the characteristics of bilateral systems, which mean stability, transparency, and scalability of bilateral control will be addressed. Then function based control that we used in our experiments will be introduced, functional control framework is analyzed for bilateral systems with simulation results.

4.2 Definitions for Bilateral Control

A definition of world bilateral means having two sides [20] [22]. Bilateral control is realization of the natural law of action and reaction between two objects. In robotics literature; bilateral control means a synchronized control system composed of two sides named master and slave side behaving interactively with each other by means of position and force as illustrated in Figure 4-1. The goal of bilateral systems to provide the extension of an operator's sensing and manipulation capability to a remote location. In one implementation, slave is required to track master's position as directed by operator and the force of interaction with environment on the slave side is to be transferred to the master as a force opposing its motion, therefore causing a "feeling" of the environment by the operator. Transparency is crucial to any bilateral controller after the stability of the overall system is guaranteed [15] [23].

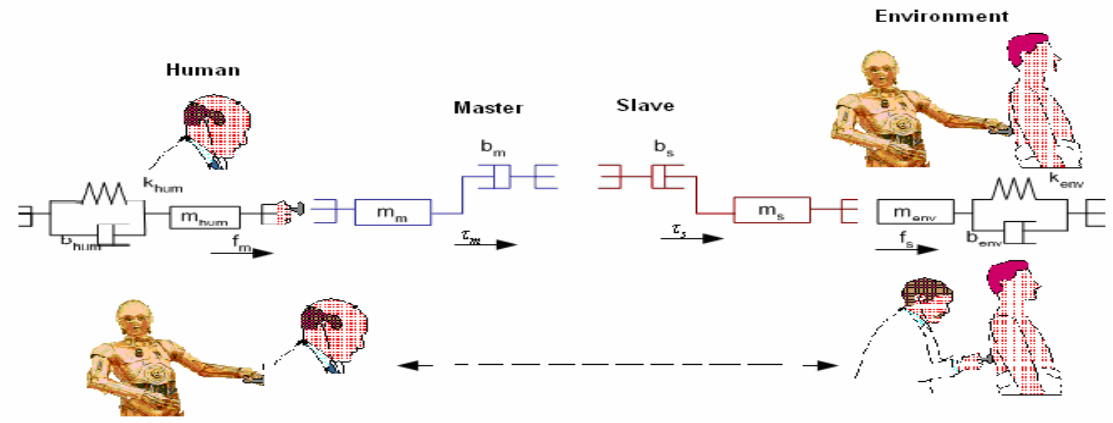

Figure 4-1– Structure of bilateral systems

In the literature the terms; bilateral control, haptics and teleoperation creates confusion about their definitions. The reason for that is; people from different areas for similar concept and different context use the same terms. In this study, the definitions are used for these terms are:

Teleoperation: Teleoperation indicates operation of master and slave robots in remote environment. Controlling the space robots movements from the earth can be given as an example, Figure 4-2.

Bilateral: Bilateral control is bidirectional control of force and position on the slave-master manipulators. Master and slave should be distant from each other; robotic surgery can be an example like in Figure 4-2. Bilateral control should transfer the

feeling of the touch from environment to the master side and in this sense, it is often perceived as a haptic system.

Haptics: Haptic, from the Greek (*Haphe*), means pertaining to the sense of touch [24]. The common ability of haptics is force sensation to the human operator comes by using haptic interfaces. Some examples are simulations, games, rehabilitation devices, Figure 4-2, [43] [45].

Teleoperation [16] Haptic [41] Bilateral [42]

Figure 4-2 – Teleoperation, bilateral, haptics

4.2.1 Characteristics of Ideal Bilateral Systems

Ideal response of a bilateral system is defined in [25] [26] as stability, transparency. They are the basic qualities that define the characteristics of ideal bilateral systems.

In this study, communication delay is out of consideration and the variables those are used to define system requirements are listed in Table 4-1.

Bilateral control system considers; human, environment, master – slave robots and communication channel as mentioned before. The impedances Z_h and Z_e [27] are used to symbolize human and environment. They are modeled by spring and damper system (29), (31). Figure 4-3 represents the two-port model of bilateral system in terms of effort (force) and flow (velocity).

Parameters	Descriptions
F_h	Master generated force
F_e	Slave generated force
F_m	Generated force for master manipulator
F_s	Generated force for slave manipulator
F_{md}	Disturbance force for master manipulator
F_{sd}	Disturbance force for slave manipulator
M_m	Mass of master manipulator
M_s	Mass of slave manipulator
x_m^{ref}	Position reference for master manipulator
x_m	Position of master manipulator
x_s^{ref}	Position reference for slave manipulator
x_s	Position of slave manipulator
$\dot{x}_m$	Velocity of master manipulator
$\dot{x}_s$	Velocity of slave manipulator
$\ddot{x}_m$	Acceleration of master manipulator
$\ddot{x}_s$	Acceleration of slave manipulator
i_m	Current input for master
i_s	Current input for slave
i_h	Human generated current input for master
V_h	Velocity of human
V_e	Velocity of environment

Table 4-1- Parameters of master / slave manipulators

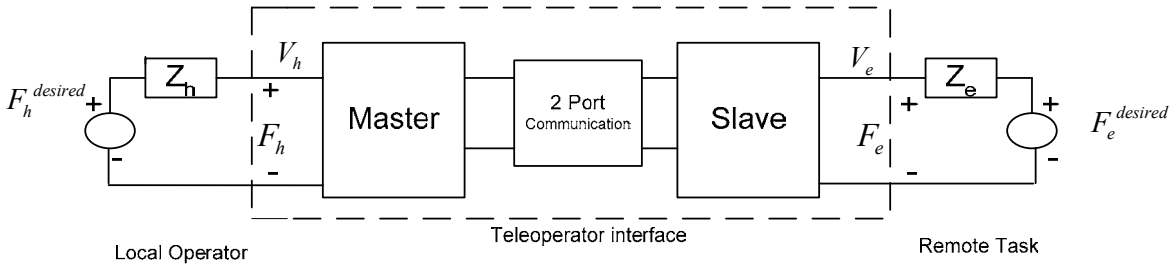

Figure 4-3– General two port model of a bilateral teleoperation system [28]

Interaction force on the environment side:

$$Z_e = C_e + D_e s \tag{29}$$

$$F_e = Z_e(x_s - x_e) \tag{30}$$

The same relation can be used for the operator side:

$$Z_h = C_h + D_h s \tag{31}$$

$$F_h = Z_h x_h \tag{32}$$

4.3 Function Based Control for Bilateral Systems

In this section, bilateral control was designed and simulated in the function based control framework. The human operator defines the tasks to be performed by the system and if there is an interaction of the slave manipulator with the environment, the operator gets force-feedback. Master manipulator takes the task data, gives the position command to the slave manipulator and besides takes remote site information from the slave, and exerts force on the operator. The master can be a joystick, a tactile device or a surgical instrument handle [27] [28] [29]. Slave manipulator takes the user's tasks from the master manipulator and realizes them in the environment while transmitting the relevant information of task development from environment to the master. It can be any robot with or without sensors to convey environment information.

Mechanical design of master and slave side of bilateral system setup is shown in Figure 4-4.

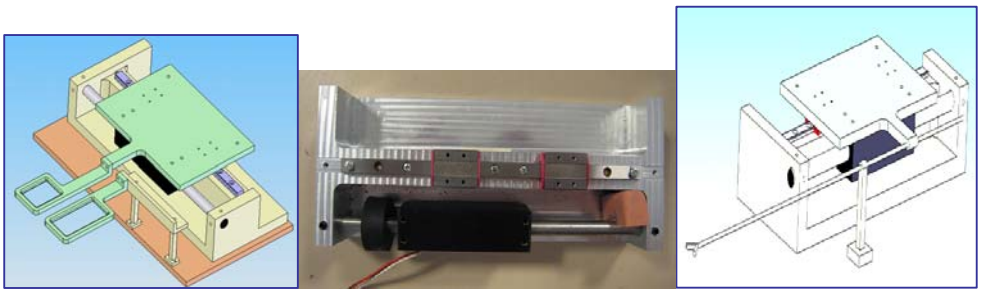

Figure 4-4 - Master manipulator Slave manipulator

Assume two single dof mechanical systems defined by (33) one of the acting as a master system and other one as a slave system.

$$m_{ii}\ddot{x}_i + n_i\left(x_i, \dot{x}_i\right) = F_i - F_{exti} \quad i = m,s \tag{33}$$

In bilateral control a specific functional relation between master and slave systems is established. That functional relation in literature is defined as $x_s = x_m$ and $F_m = -F_s$. Behavior of ideal bilateral system is defined as requirement that error in position (34) and the error in force (35) are zero.

$$\varepsilon_{x-}(t) = x_m(t) - x_s(t) \tag{34}$$

$$\varepsilon_{F+}(t) = F_s(t) + F_m(t) \tag{35}$$

There are many possible ways to approach design of control on master and slave side. In control system design, for single DOF identical master and slave systems are performed applying disturbance feedback so that master and slave subsystems are represented as $\ddot{x}_i = F_i \quad i = m,s$ and then the acceleration controller can be designed for plants (36) and (37).

$$\begin{aligned} \ddot{\varepsilon}_x &= \ddot{x}_m - \ddot{x}_s \\ \ddot{\varepsilon}_x &= F_m - F_s, \ \ddot{\varepsilon}_x = F_x \end{aligned} \tag{36}$$

$$\ddot{\varepsilon}_F = \ddot{x}_m + \ddot{x}_s$$
$$\ddot{\varepsilon}_F = F_m + F_s, \ddot{\varepsilon}_F = F_F \tag{37}$$

Now selection of F_x and F_F is a simple task and the real control inputs are easily obtained as: $F_m = \frac{1}{2}(F_x + F_F)$ and $F_s = \frac{1}{2}(F_F - F_x)$. In this approach the design is performed in very similar way as standard SMC is done. Namely the original plant is projected in the new subspace in which the control inputs are selected and then control is projected back to the original state space. The result can be extended to systems like microsystems with scaling between master and slave side and to multilateral control creating new functions between multi-elements.

In the framework proposed in this study the subspace in which control is synthesized is defined by selection of manifold defined as a difference between actual and desired configuration of the system (8).

In bilateral control system, consisting of functionally related master and slave subsystems, manifold should be selected as an intersection of the position tracking (38) and force tracking (39) manifolds.

$$S_x = \left\{ (x_m, x_s) : \ \xi_m(x_m, \dot{x}_m) - \xi_s(x_s, \dot{x}_s) = \sigma_x = 0 \right\} \tag{38}$$

$$S_F = \left\{ (x_m, x_s) : \ F_{\mathrm{h}}(x_m, \dot{x}_m) + F_e(x_s, \dot{x}_s) = \sigma_F = 0 \right\} \tag{39}$$

Master side requirement can be rearranged taking account the human operator and environment impedances as follows:

$$S_F = \left\{ (x_m, x_s) : \ \left(C_h x_m + D_h \dot{x}_m \right) + \ \left(C_e x_s + D_e \dot{x}_s \right) = \sigma_F = 0 \right\} \tag{40}$$

In the above formulation the coefficients C_h and D_h can be selected in such a way that impedance perceived by the human operator is scaled in order to give a feeling of a virtual tool in operator's hand. Scaling gains importance particularly for cases in which characteristic impedance of the task and the operator are very different from each other like micromanipulation where forces in the micro scale are different from the operator perception.

Bilateral control is achieved on the intersection of the above manifolds:

$$S_B = \left\{ \left(x_m, \dot{x}_m, x_S, \dot{x}_S \right) :\ S_{\mathrm{X}} \cap S_F, \sigma_x \cap \sigma_F = 0 \right\} \tag{41}$$

By defining errors (34) and (35), (38) and (40) can then be expressed as follows

$$S_x = \left\{ \left(x_m, x_S \right) : Q\dot{\varepsilon}_x + G_x \varepsilon_x = \sigma_x = 0 \right\} \tag{42}$$

$$S_F = \left\{ \left(\varepsilon_{x+}, \dot{\varepsilon}_{x+}, x_S \right) : C_h \varepsilon_{x+} + D_h \dot{\varepsilon}_{x+} + \left(C_e - C_h \right) x_S + \left(D_e - D_h \right) \dot{x}_S = \sigma_F = 0 \right\} \tag{43}$$

$$\varsigma\left(x_s, \dot{x}_s \right) = \left(C_e - C_h \right) x_S + \left(D_e - D_h \right) \dot{x}_S \tag{44}$$

Disturbance observer can be put the system to eliminate either external forces or disturbances (44) on the system.

Now projection of the system motion in the selected manifolds can be expressed as

$$\dot{\sigma}_x = Q\ddot{\varepsilon}_x + G_x \dot{\varepsilon}_x \tag{45}$$

$$\dot{\sigma}_F = Q_x \left[\left(\frac{1}{m_m} F_m + \frac{1}{m_S} F_S \right) - \left(\frac{1}{m_m} d_m - \frac{1}{m_S} d_S \right) \right] + G_x \dot{\varepsilon}_x \tag{46}$$

$$\dot{\sigma}_F = \left(D_h \ddot{\varepsilon}_{x+} + C_h \dot{\varepsilon}_{x+} \right) + \varsigma\left(x_S, \dot{x}_S \right) \tag{47}$$

$$\dot{\sigma}_F = D_h \left[\left(\frac{1}{m_m} F_m + \frac{1}{m_s} F_s \right) - \left(\frac{1}{m_m} d_m + \frac{1}{m_s} d_s \right) \right] \varsigma(x_s, \dot{x}_s) \tag{48}$$

Equations (46) and (48) can be rewritten as $\dot{\sigma}_x = i_{\varepsilon x-}$ and $\dot{\sigma}_F = i_F$, respectively. These equations represent two simple first order systems and selection of control enforces stability in intersection (41).

4.4 Bilateral Control Simulation Results

4.4.1 Position Control

In this part of study, we concentrate on equation (34) which tells the slave side should follow the position of the master side precisely. Conventionally, position of master manipulator will be reference for slave manipulator, and controller makes position error zero.

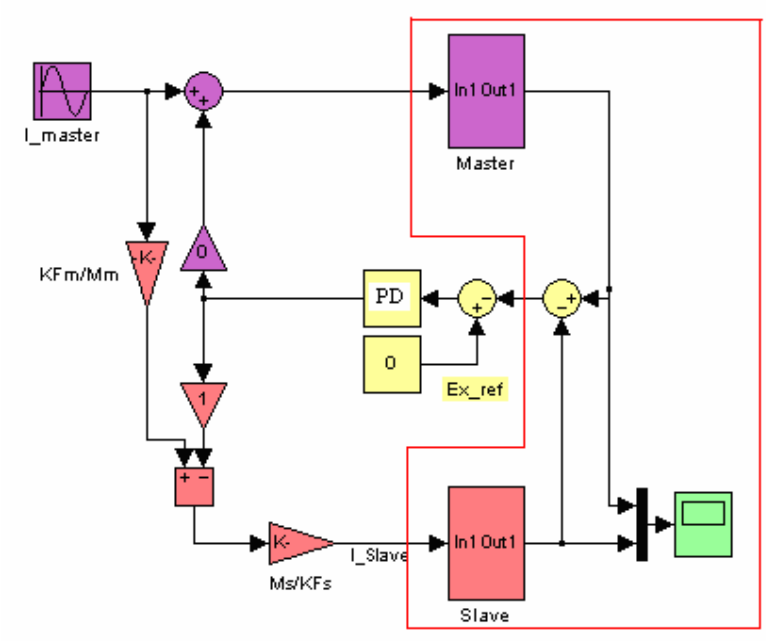

Figure 4-5 – Position control block diagram (ε_{x-})

This is second order system and the stability criterion is known, so that we choose PD controller, which has well enough capability of controlling positions as discussed in the previous section.

Parameters used in the position control analysis are shown in Table 4-2.

Parameters	Descriptions	Values
M_m	Inertia about master motor shaft	16.9×10^{-3} kgm^2
M_s	Inertia about slave motor shaft	16.9×10^{-3} kgm^2
K_{Fm}	Force coefficient of master motor	11×10^{-3}
K_{Fs}	Force coefficient of slave motor	11×10^{-3}
K_p	Proportional control	13.7728
K_d	Derivative control	0.0599

Table 4-2- Parameters used in position control analysis

Master control input is given directly and control input for the slave is calculated using (36).

The position response to (34) is shown in Figure 4-6 and Figure 4-7 with $i_h = 1\times10^{-4}\times(\sin\omega t)$, with $\omega t = \frac{\pi}{3} rad/\sec$. Error between the reference ε_{x-}^{ref} and ε_{x-} is zero.

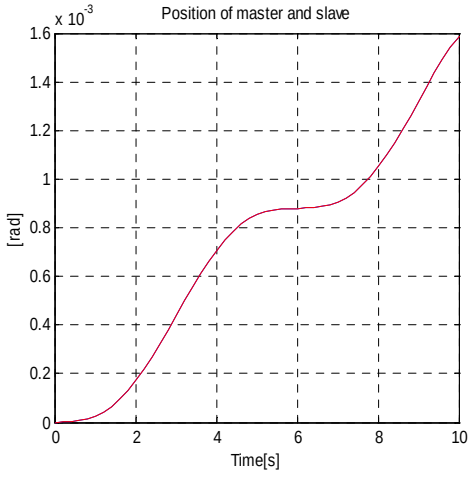

Figure 4-6 - Positions of master-slave

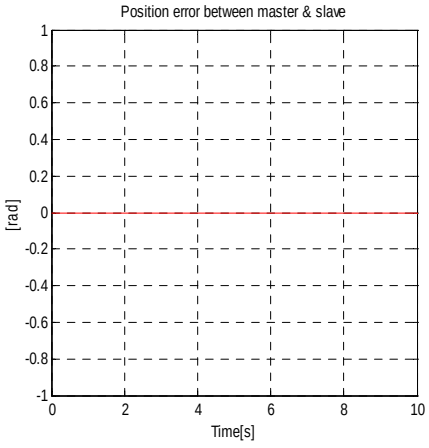

Figure 4-7 - Position error between master-slave

The results show that position is well controlled. Master and slave robots have same impedances so that they perfectly track each other. The simulation results show that we can implement this architecture for position control.

4.4.2 Force Control

Control objective of this section is to find control in such a form that the force controller error $\varepsilon_{F+} = F_m + F_s$ has stable zero value. Figure 4-16 shows the force control block diagram.

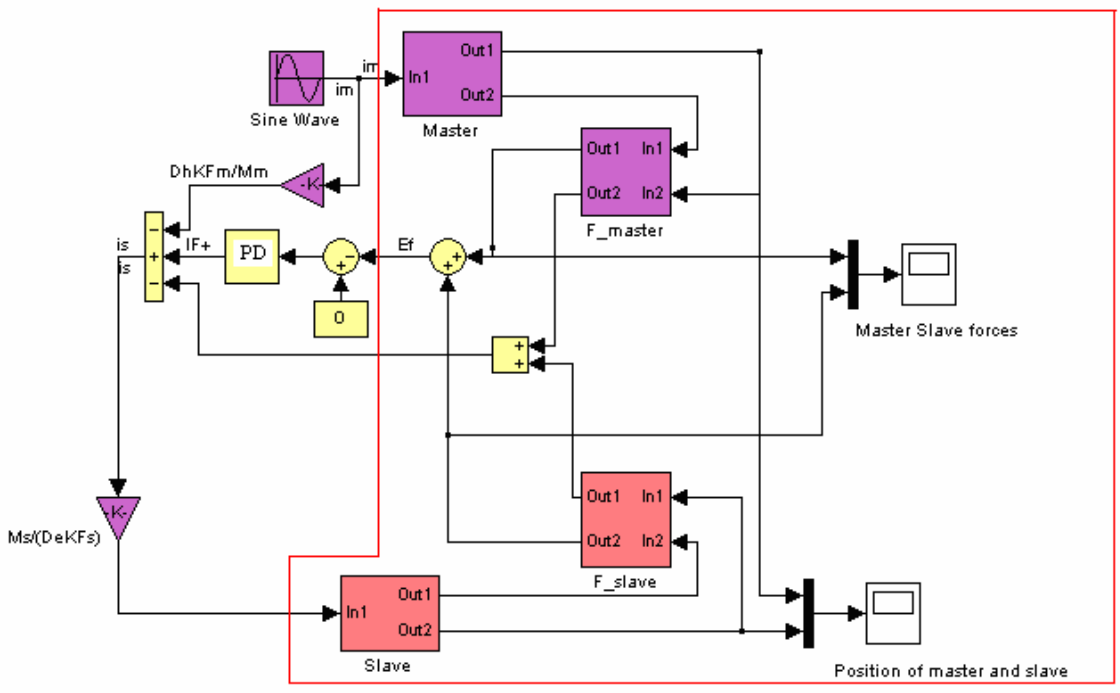

Figure 4-8 –Force control block diagram

Parameters are used in the force control analysis are shown in Table 4-3.

Force Estimating Parameters	Values
C_h	0.1555 N/m
C_e	0.17658 N/m
D_h	0.0111 Ns/m
D_e	0.03476 Ns/m
Controller Parameters	**Values**
K_p	100
K_d	0.04

Table 4-3 – Parameters used in force control analysis

The force response to (35) is shown in Figure 4-9 with $i_h = 1\times10^{-4}\times(\sin\omega t)$, with $\omega t = \frac{\pi}{3} rad/\sec$. Error between the reference ε_{x-}^{ref} and ε_{x-} is very small.

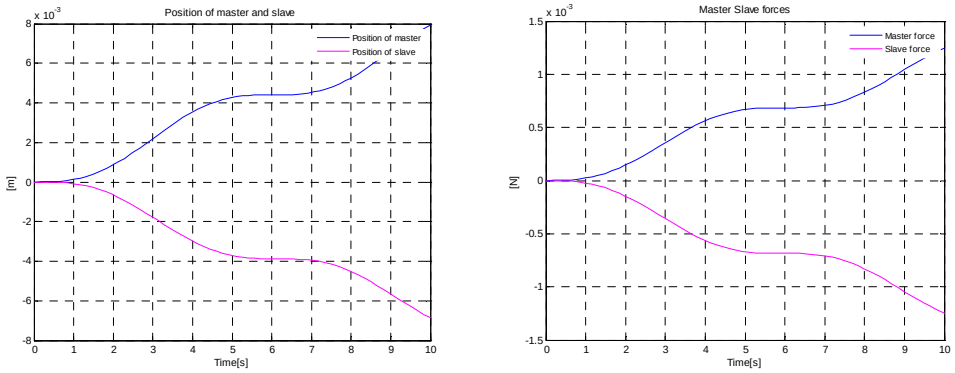

Figure 4-9 – Positions of master-slave - Forces of master-slave

Force of master and slave manipulator is scaled version of position as seen Figure 4-9.

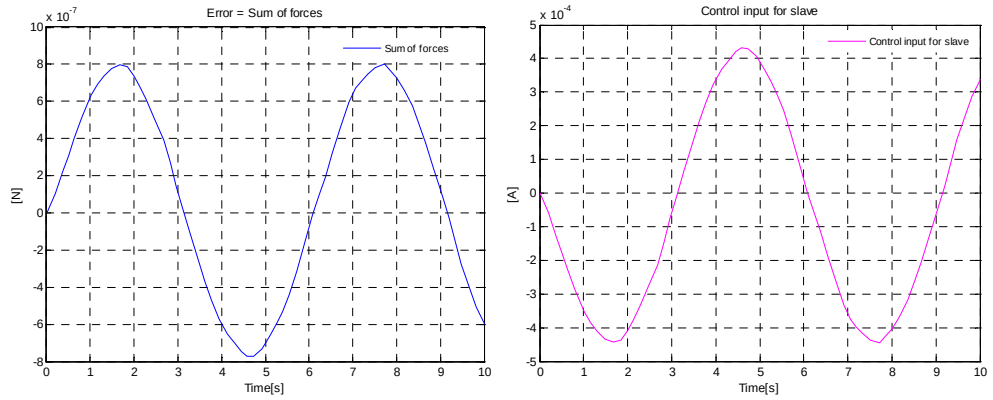

Figure 4-10 – Error – Control input

The results show that position and forces are controlled when decoupled. Sum of master and slave system's position is controlled and error is $-8\times10^{-5}N$ so that forces are equal and have opposite signs as seen from Figure 4-9. The second requirement of bilateral system is occurs. The simulation results show that this architecture can be used as a major part of force controller design.

In addition to that, environmental force is generated by slave robots interaction (position changing) with an obstacle. The purpose of this part is to show that the environmental force is equal to the slave side force based on spring-damper model of

environment and force of master side is equal to the slave side force reference with opposite sign.

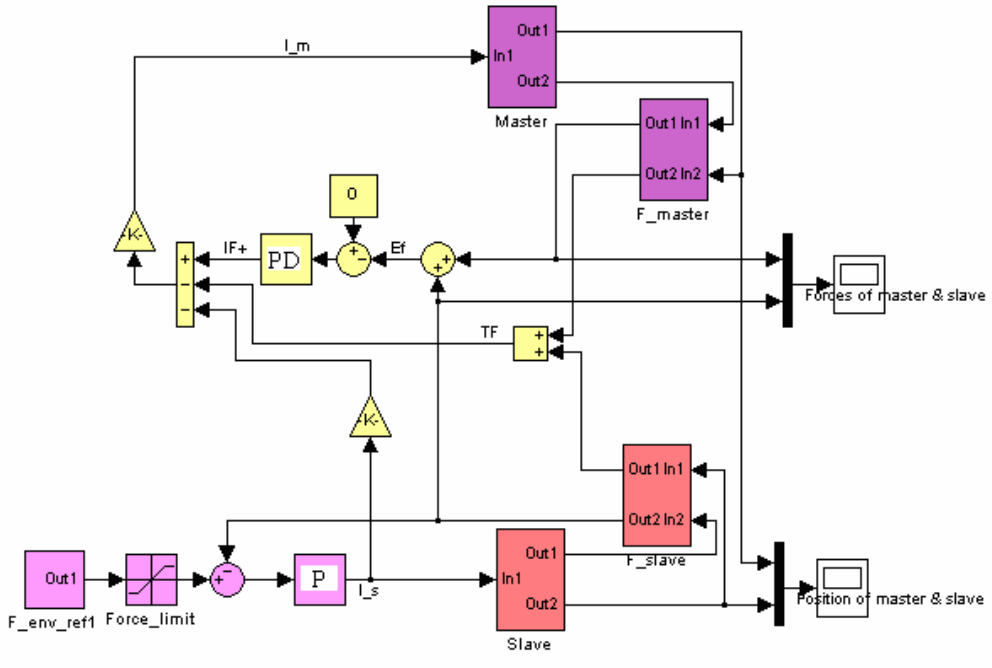

Figure 4-11 – Block diagram for force control based on slave control input

Parameters	Values
P Controller	
K_p	2.5
PD Controller	
K_p	10
K_d	0.888999
Force Limit	Upper limit: 1
	Lower limit: -1

Table 4-4 – Parameters used in force control analysis

Action and reaction forces are seen in Figure 4-12 with respect to the positions of master and slave. It shows one of the ideal bilateral control conditions

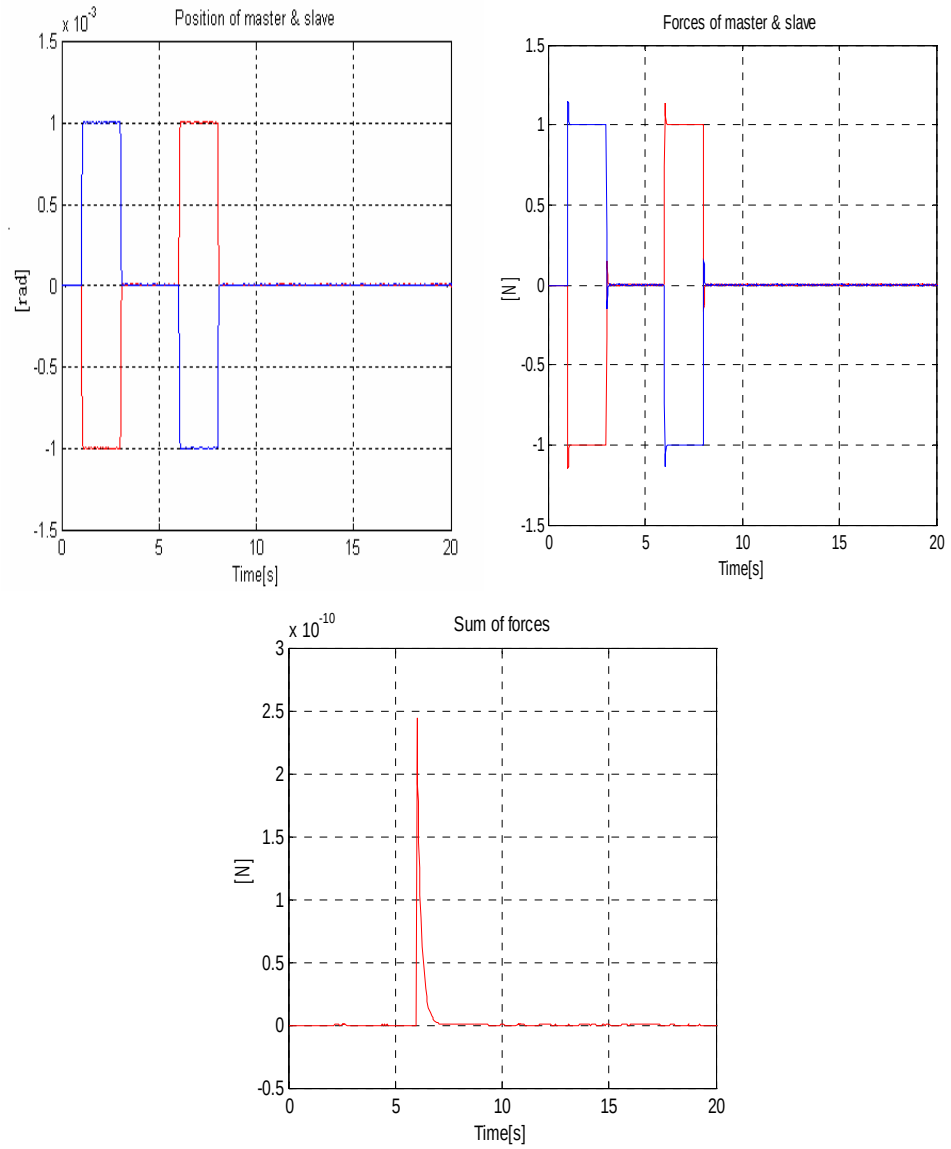

Figure 4-12 – Position, forces and sum of forces of master-slave manipulators

4.4.3 Sliding Mode Control of Bilateral Systems

The scenario used for the simulation is such that operator gives force to the master manipulator so that position of the master robot changes. Master robot's position becomes position reference for the slave manipulator. Therefore, control task is defined as $\varepsilon_{x-} \to 0$. A sinusoidal obstacle created in the slave's environment and interaction force exists on the slave manipulator as a function of obstacle. When slave contacts with

environment, interaction force is generated and it becomes force reference for the master manipulator. Control objective for forces is $\varepsilon_F \to 0$.

With respected to the above scenario, two simulation results are presented. For the first one human and environment have the same impedances, while the second one has different values shown in Table 4-5.

Simulation_1		
Spring coefficient(C) Damper(D)	Operator and Environment	$C_h = C_e = 0.17658$ N/m $D_h = D_e = 0.03476$ Ns/m
Simulation_2		
Spring coefficient(C) Damper(D)	Environment Operator	$C_e = 0.17658$ N/m $D_e = 0.03476$ Ns/m $C_h = 0.1555$ N/m $D_h = 0.0111$ Ns/m

Table 4-5 – Impedance for human and environment

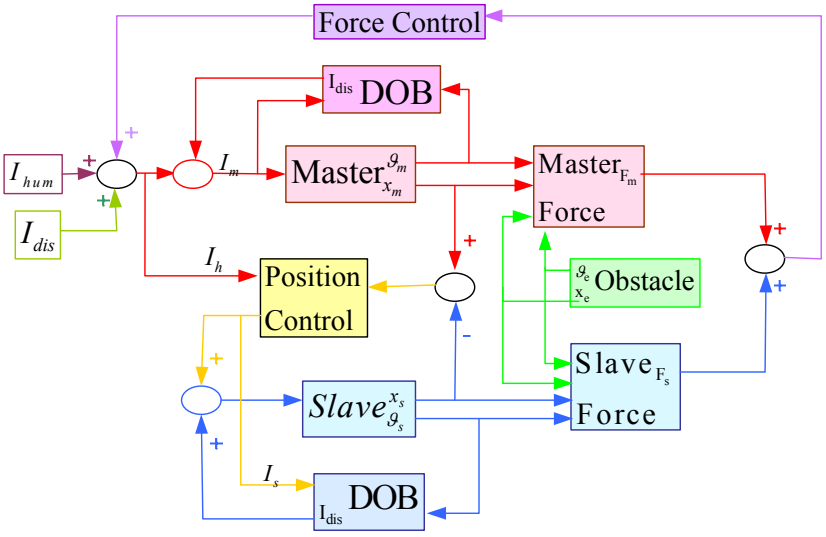

Figure 4-13 – Block diagram for bilateral architecture

Simulation block diagram is illustrated as in Figure 4-13 and controller parameters are shown in Table 4-6.

Parameters	Values
C	30
D	1000
Ku	0.000001

Table 4-6 – Parameters used in Sliding mode controller

Simulation I: Master-slave positions and forces with an obstacle are illustrated in Figure 4-14. The relationship between obstacle and forces is wanted to emphasize. If there is no interaction between robots position and obstacle, force does not exist. System response between the 30 and 48 seconds can be an example for this situation.

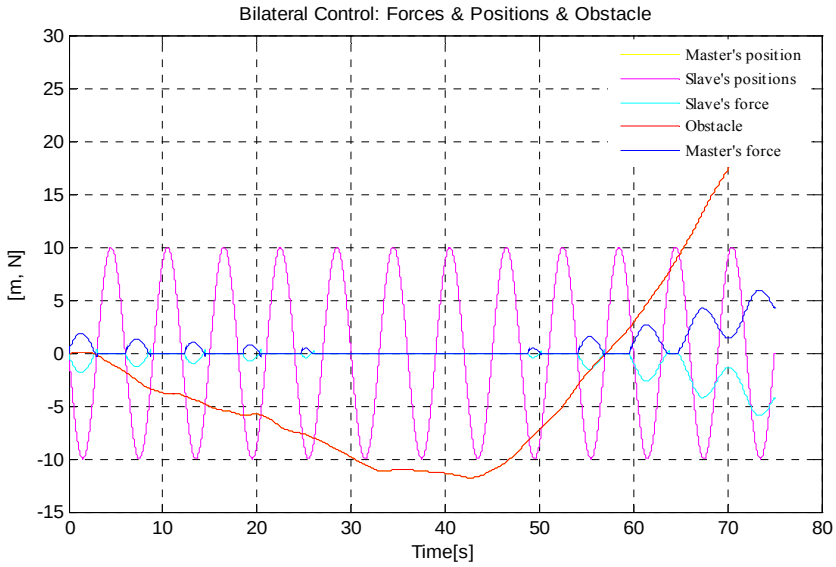

Figure 4-14 – Bilateral control: forces, positions and obstacle

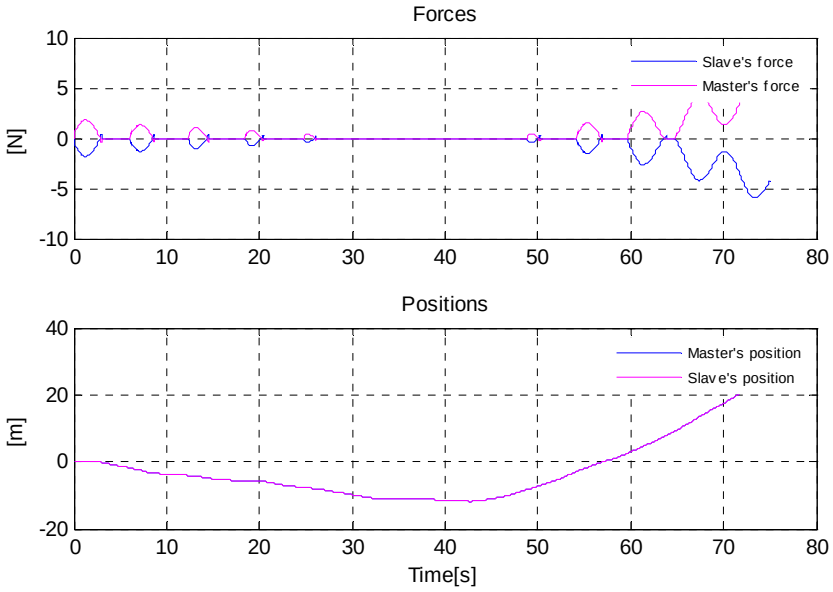

Figure 4-15 - Forces

Impedance values used to model human and environment are same, so that forces on master and slave have the same magnitude and opposite signs as expected. Position tracking performance is also satisfactory. Figure 4-15 shows the system responses.

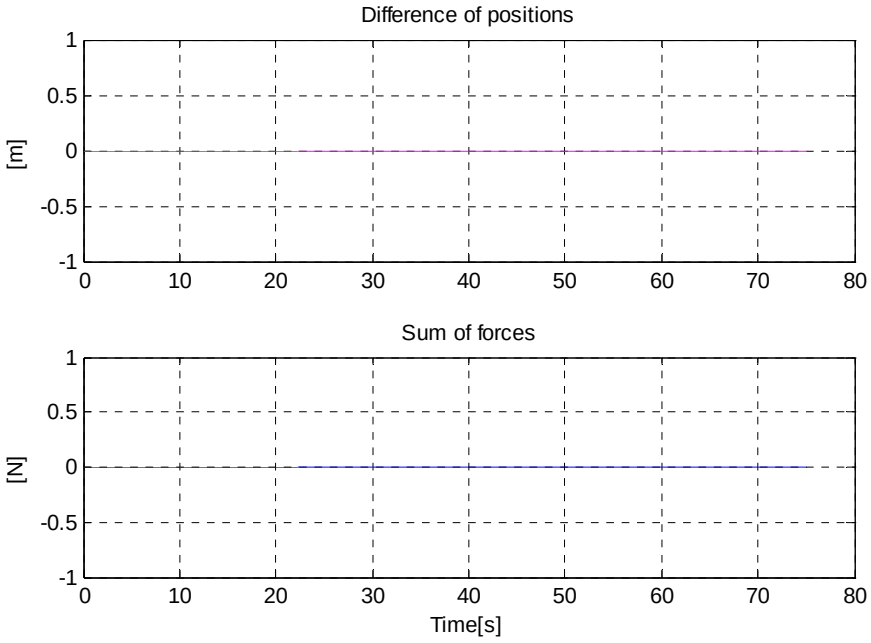

Figure 4-16- Errors

Figure 4-16 shows that $\varepsilon_{X-} \to 0$ and $\varepsilon_{F+} \to 0$.

Simulation II: Figure 4-17 shows the simulation results with different impedance value for environment. In this figure, positions are on the position limit, so that they are 1000 and do not change. There is a control on the forces. The obstacle model is as the same as previous simulation model.

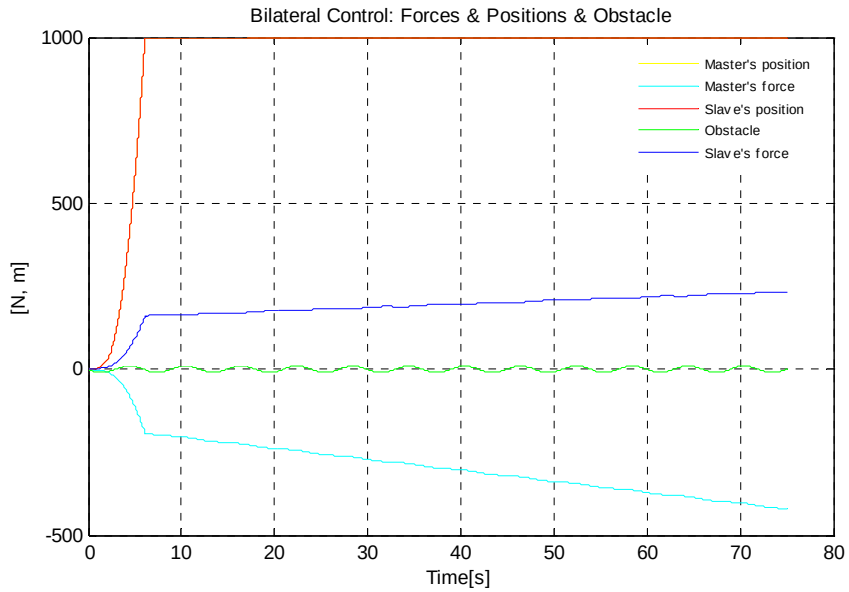

Figure 4-17 - Bilateral control: forces, positions and obstacle

Figure 4-26 shows errors between master and slave positions and forces. Sum of forces is not zero at the beginning, after a few seconds it becomes zero.

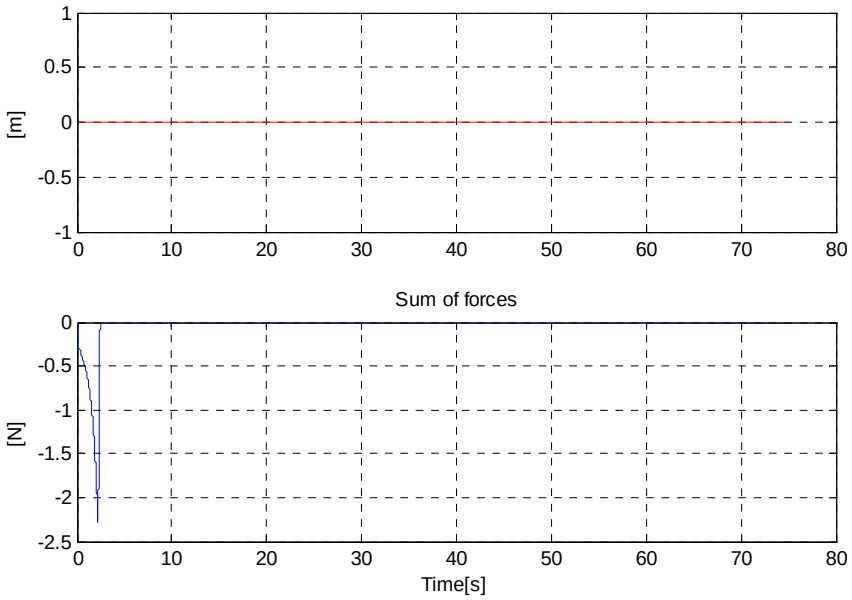

Figure 4-18 – Error

In simulations, position tracking and force transparency are achieved. All signals are bounded and error becomes zero. The results of both position and force control are

satisfactory. So, functional control framework can be applied on bilateral systems. The simulation results prove that this control algorithm can be implemented.

5 PARALLEL MECHANISMS

5.1 Introduction to Parallel Mechanisms

Parallel type manipulators have been more popular since 1980's due to their high force loading capacity and fine motion characteristics in terms of stiffness, accuracy, speed and payload are over their serial counterparts because of their closed looped mechanisms. Researchers try to utilize all these advantages to develop high precision tools and dexterous devices which can be used in industry or in nanotechnology or in biotechnology fields.

The historical background of the parallel mechanisms are based on Gough-Stewart platform, originally design as an aircraft simulator then used in different areas. The aim of this study is to observe the effectiveness of functional control approach for parallel mechanisms like pantograph and three-legged robot. Investigated parallel mechanisms are designed to be used as parts of micro assembly workstation due to their advantages. Parallel type robots consider closed kinematic chains only and every kinematic chain includes both active and passive kinematic pairs, [30]. Intention of study is as the same as bilateral control systems; to divide desired motion into tasks and design simple controllers.

The structure of the chapter is first, a general description, advantages and disadvantages of parallel mechanisms will be addressed. Then some control methods are examined for pantograph and three – legged robot with function based control and results will be compared via simulations.

5.2 Definition of Parallel Mechanisms

"A parallel robot is made up of an end-effector with n degrees of freedom, and of a fixed base, linked together by at least two independent kinematic chains. Actuation takes place through n simple actuators" is definition of parallel robots by [31].

[30] and [32] discussed the advantages and disadvantages of parallel manipulators as follows:

The advantages of the parallel mechanisms are:

-high rigidity,

-high payload-to-weight ratio,

-high accuracy,

-low inertia of moving parts,

-high agility,

-inverse kinematics problem has simple solution.

The disadvantages of the parallel mechanisms are:

-limited work volume,

-low dexterity,

-complicated direct kinematic solution,

-singularities that occur both inside and on the envelope of the work volume.

Parallel manipulators share the load by several kinematic chains results in high payload to-weight ratio and rigidity. The high accuracy stems from sharing, not accumulating, joint errors. The best suitable implementation of parallel mechanisms includes requirements for limited workspace, high accuracy, high agility, and a lightweight and a compact robot.

5.3 Pantograph

The goal of this section is to control the pantograph by function based controllers, which is one of the promising areas of decentralized control field.

In our case, five-bar linkage, including some challenging characteristics is investigated. The known features of parallel manipulators, which consists of a closed kinematics chains, have good positioning capability [33] therefore the pantograph is chosen for miniaturization for micro assembly tasks. However, some disadvantages

exist, because of their parallel topology, it is difficult to analyze, synthesize, control and plan trajectories. Function based control is adopted to solve these advantages.

In this section, kinematic and dynamic model of the system is calculated and is modeled and simulated in [33] using Simmechanics blocks (MATLAB). Pantograph is controlled via classical and functional control techniques and results are presented.

Figure 5-1- Pantograph

Designed pantograph for this study is a three degree of freedom ($XY\theta$) parallel mechanism with optimized link lengths (a_1, a_2, a_3 a_4, a_5) [35],]. P_1 and P_2 are actuated, fixed joints, while P_3 and P_5 are passive joints. The tip of the pantograph is represented by P_4 and all joints are revolute. Necessary degrees of freedom for the pantograph are three; two translational axes to allow the work piece to be positioned in X and Y orthogonal axes and an independent rotational axis in order to orientate the work piece under the microscope. In the following figure link lengths and dexterous workspace of 20 mm x 20 mm square are shown.

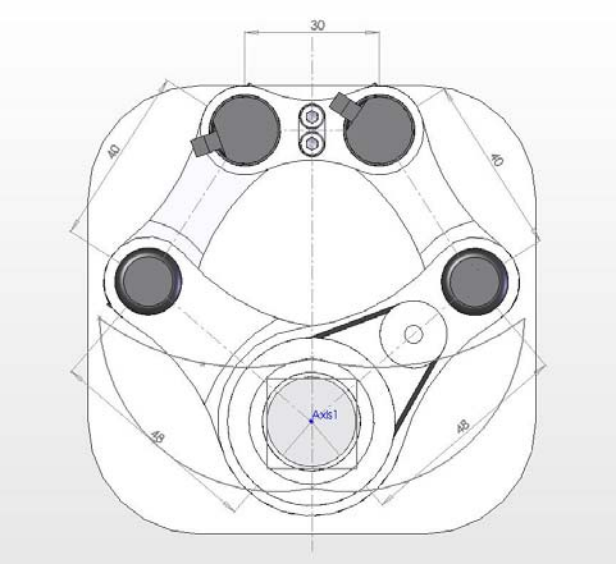

Figure 5-2 – Workspace and link lengths

Micro assembly applications need very high accuracy, so that precision and repeatability for this system changes in the micron to nanometer range, enough resolutions are 1micro meter for XY motion and 0.001 degree for the rotary motion.

5.4 Kinematics of Pantograph

5.4.1 Forward Kinematics

Forward kinematics is used to find the end point P_4 position of the pantograph corresponding to the given actuated joint angles θ_1 *and* θ_2. The geometric approach is explained in the Figure 5-3.

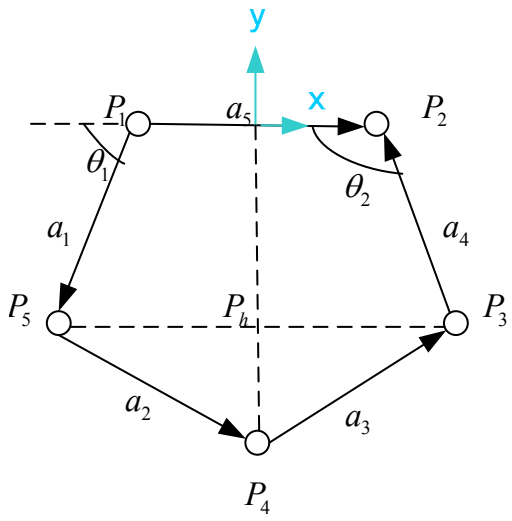

Figure 5-3 - Geometric representation for forward kinematics

Calculation of forward kinematics based on geometric approach is derived as [33].

$$P_5(x_2, y_2) = \left[-a_1 \cos\theta_1 - \frac{a_5}{2},\ -a_1 \sin\theta_1 \right]^T \tag{49}$$

$$P_3(x_4, y_4) = \left[a_4 \cos\theta_5 + \frac{a_5}{2},\ -a_4 \sin\theta_5 \right]^T \tag{50}$$

$$\|P_5 - P_h\| = \frac{(a_2^2 - a_3^2 + \|P_3 - P_5\|^2)}{(2\|P_3 - P_5\|)} \tag{51}$$

$$P_h = P_5 + \frac{\|P_5 - P_h\|}{\|P_5 - P_3\|}(P_3 - P_5) \tag{52}$$

$$\|P_4 - P_h\| = \sqrt{a_2^2 - \|P_5 - P_h\|^2} \tag{53}$$

$$x_4 = x_h + \frac{\|P_4 - P_h\|}{\|P_5 - P_3\|}(y_3 - y_5) \tag{54}$$

$$y_4 = y_h - \frac{\|P_4 - P_h\|}{\|P_5 - P_3\|}(x_3 - x_5) \tag{55}$$

5.4.2 Inverse Kinematics

Goal of inverse kinematics is to find actuated joints θ_1 and θ_2, given the end point position P_4. Position control of P_4 requires to define reference actuated joint angles to the motors. P_5 and P_3 are passive joints so their positions can not be measurable, as a result their positions are not used directly to calculate the position of P_4. Therefore, [33] developed the method using two triangles and cosines theorem as follows:

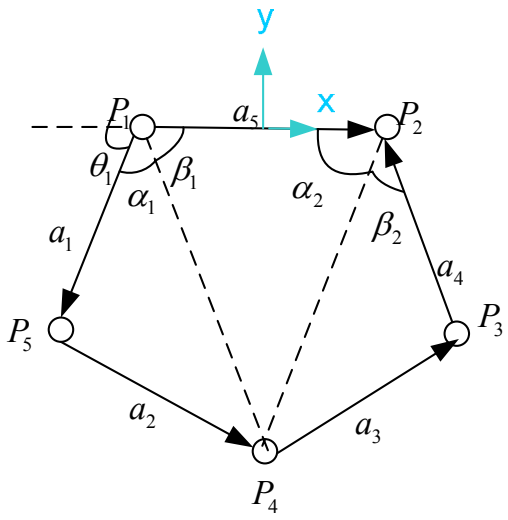

Figure 5-4 - Triangles and end point positions for inverse kinematics

Inverse kinematics of pantograph can be calculated as follows:

$$\alpha_1 = \arccos\left(\frac{a_1^2 - a_2^2 + \|P_1, P_4\|}{2a_1\sqrt{\|P_1, P_4\|}}\right) \tag{56}$$

$$\beta_1 = \text{a}\tan 2\left(y_4,\ -x_4 + \frac{a_5}{2}\right) \tag{57}$$

$$\beta_2 = \arccos\left(\frac{a_4^2 - a_3^2 + \|P_2, P_4\|}{2a_4\sqrt{\|P_2, P_4\|}}\right) \tag{58}$$

$$\alpha_2 = \text{a}\tan 2\left(y_4,\ x_4 + \frac{a_5}{2}\right) \tag{59}$$

$$\theta_1 = \pi - \alpha_1 - \beta_1,\ \theta_2 = \alpha_2 + \beta_2 \tag{60}$$

The initial theta value 63^0 where the end of the pantograph is on the world coordinates of the y axis.

$$\theta_1 = \pi - \alpha_1 - \beta_1 - a\tan 2 \tag{61}$$

$$\theta_2 = \alpha_2 + \beta_2 - (\pi - a\tan 2) \tag{62}$$

Using inverse kinematics calculation for any given x and y, θ_1 and θ_2 are found.

5.5 Modeling and Control of Pantograph

Obtaining forward and inverse kinematics gives the opportunity of using Simmechanics toolbox of MATLAB for simulation. Solidworks is used to get necessary information for Simmechanics blocks. Inertias of the link lengths are shown in Table 5-1.

Inertias	Values
M_1	$26\times10^{-3}\ kg$
M_2	$31.9\times10^{-3}\ kg$
M_3	$30.5\times10^{-3}\ kg$
M_4	$26\times10^{-3}\ kg$
M_5	$10\times10^{-3}\ kg$

Table 5-1- Inertias of link lengths

Pantograph has two dof and four joint variables θ_1 and θ_2 are independent and others are passive joints as a function of independent variables. The objective of this section is to derive all relationship between the independent variables and to control the x-y coordinates of tool tip without considering passive joints. Block diagram and composed mechanisms are illustrated in Figure 5-6 and Figure 5-5.

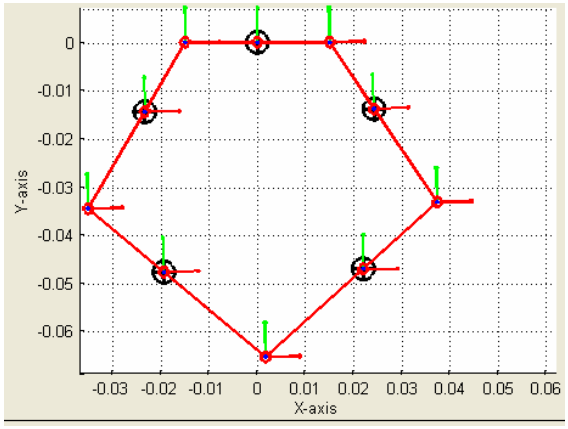

Figure 5-5 – Simulation of pantograph in Simmechanics

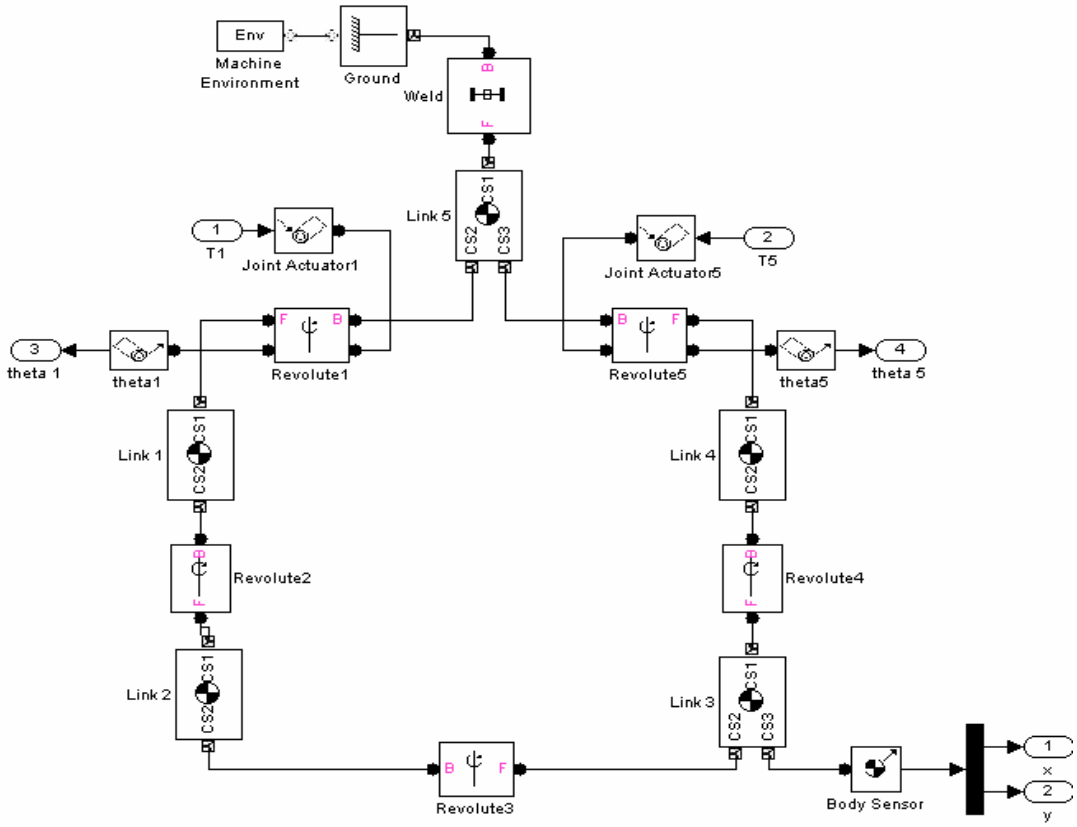

Figure 5-6 – Simmechanics model of pantograph

5.5.1 Classical control and simulation results

In this approach, the references for x-y coordinates are translated to the references for motor angles by inverse kinematics. In the inner-loop, the angles are controlled by PD controller.

Controller parameters	Values
K_p	6
K_d	0.3
Controller	Dspace 1103

Table 5-2 – Controller parameters

The parameters are taken from Faulhaber motor: 2642 012 CR series graphite commutation DC Micromotor in Table 3-1.

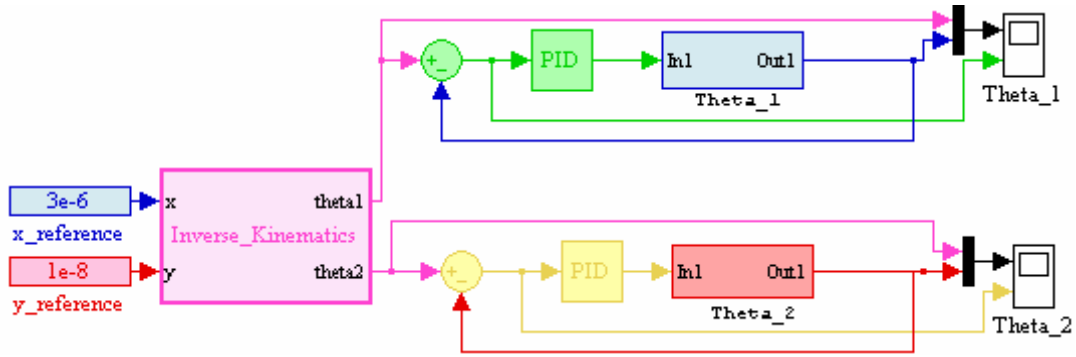

Figure 5-7 – Classical control framework

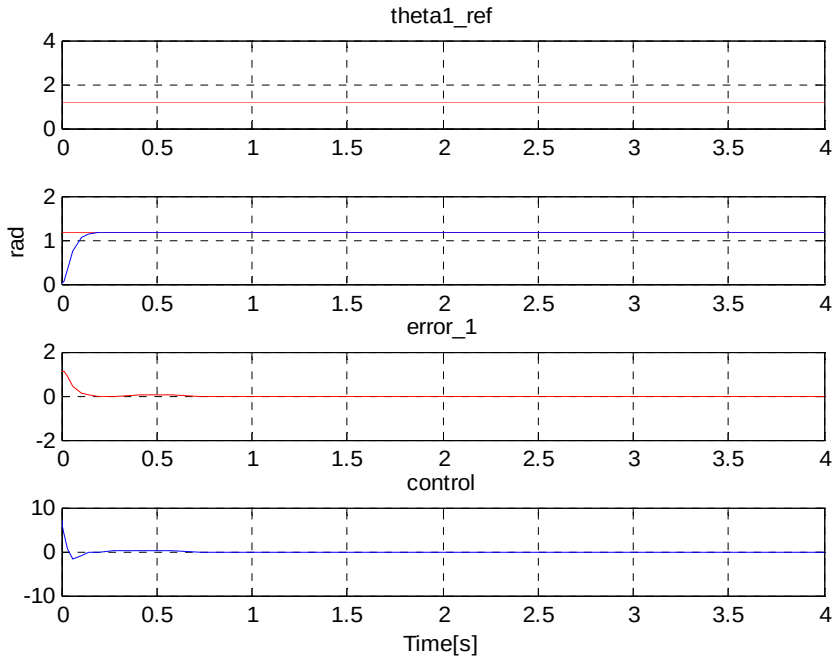

Figure 5-8 – System response for theta1

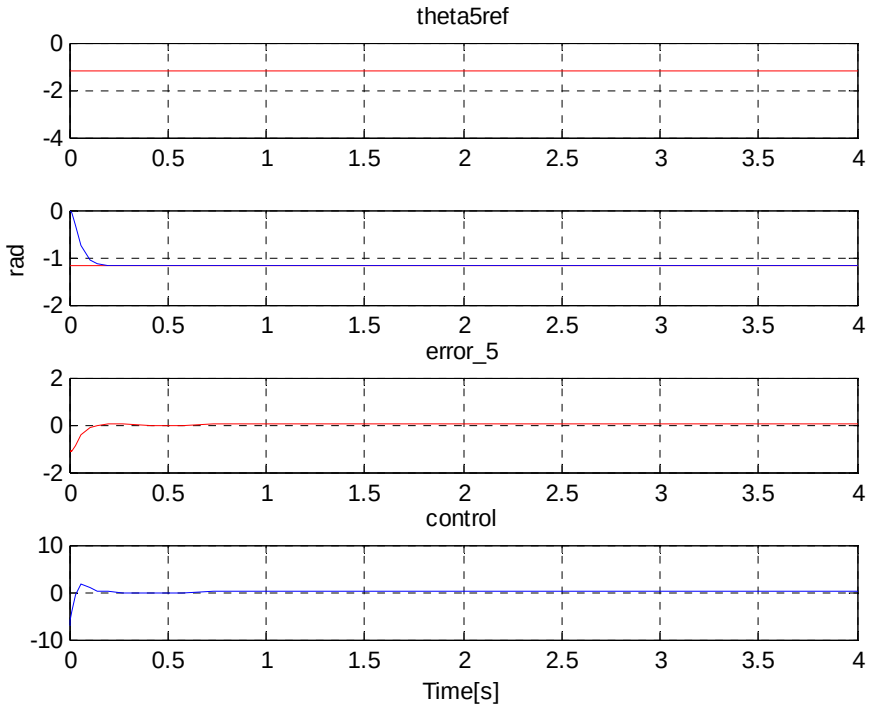

Figure 5-9 – System response for theta2

As seen in Figure 5-8 and Figure 5-9, controller works very well. There is no steady state error, rise time is very fast and there are no oscillations. The references are 3e-6 m and 1e-8 m respectively for theta1 and theta5.

5.5.2 Function based control and simulation results

Pantograph has two motions along the x-y directions. Transformation matrix should include both transformations from robot space to function space and kinematic equations from thetas to end effector.

Subsystems should be defined in order to derive relationships to compose functions. Pantograph is a closed chain mechanism so, the way is used for function based control is as follows, two planar manipulators create two subsystems which can be controlled to put the distance constant between two planar arms so we can implement rigid coupling function. Virtual objects are W and Q as shown in Figure 5-10.

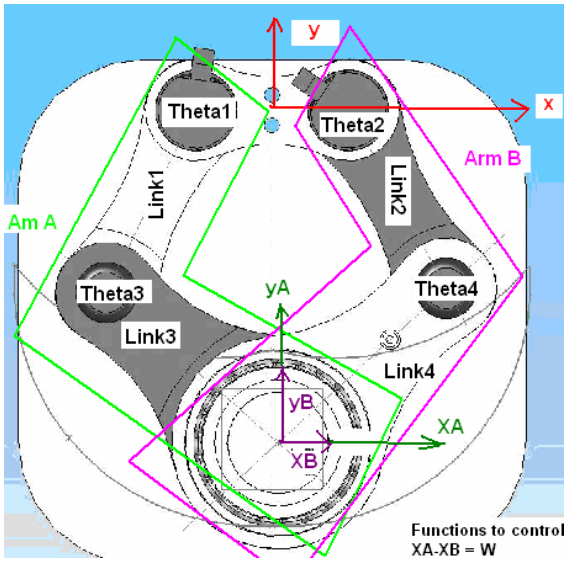

Figure 5-10 – Functions for pantograph

$$W = XA - XB,\ W = f(\theta_1, \theta_2) \tag{63}$$

$$Q = yA - yB,\ \mathrm{Q} = f(\theta_1, \theta_2) \tag{64}$$

Tool tip position of two planar manipulators is used to calculate W and Q.

$$XB = 15 + 40\cos\theta_1 + \cos(\theta_1 + \theta_3) \tag{65}$$

$$yB = -40\sin\theta_1 - 48\sin(\theta_1 + \theta_3) \tag{66}$$

$$XA = -15 - 40\cos\theta_2 - 48\cos(\theta_2 + \theta_4) \tag{67}$$

$$yA = -40\sin\theta_2 - 48\sin(\theta_2 + \theta_4) \tag{68}$$

θ_2, θ_4 are passive joints so there is no actuator to control these angles. System is under actuated, and passive joints create some problems about controlling the system. In fact, this kind of study has done [18], [34] for fully actuated parallel robots. If it is a 1 dof system (motion exists only on the x direction or y direction) the relationship between variables in robot coordinates and virtual coordinates are defined:

$$\begin{aligned} X_{f1} &= X_{r1} \\ X_{f1} - X_{f2} &= X_{r2} \end{aligned} \tag{69}$$

And corresponding transformation matrix is as follows:

$$T = \begin{bmatrix} 1 & 0 \\ 1 & -1 \end{bmatrix} \tag{70}$$

In this transformation matrix, the first function is position limit function due to the priority ordered tasks. It helps end point to stay in the defined workspace and supply safety.

In order to give reference for both x and y direction, rigid coupling function should be used for both arms, so that number of functions are three with position limit controller. In this approach, the number of controller should be equal the number of system freedom.

Step _1: In the following simulink model considers only one reference which means only x reference or y reference can be given at the same time.

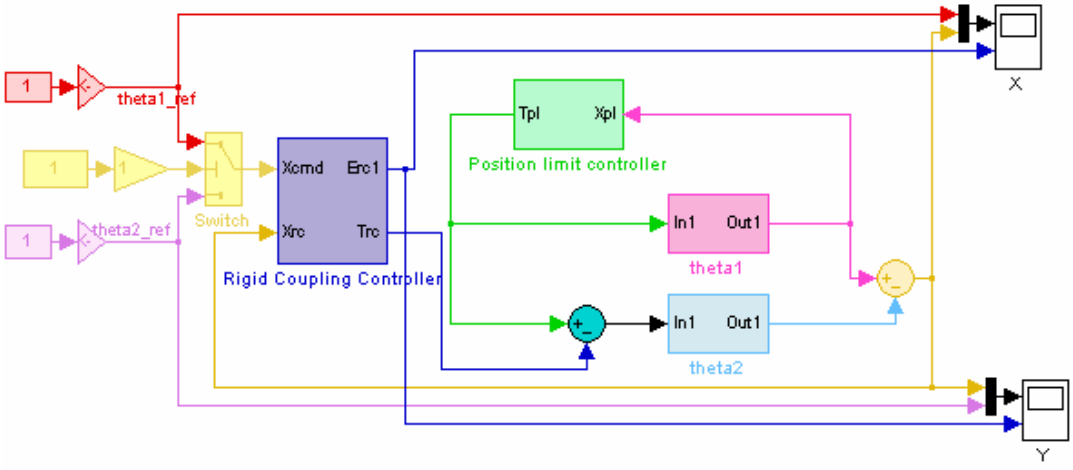

Figure 5-11 – Step_1 block diagram

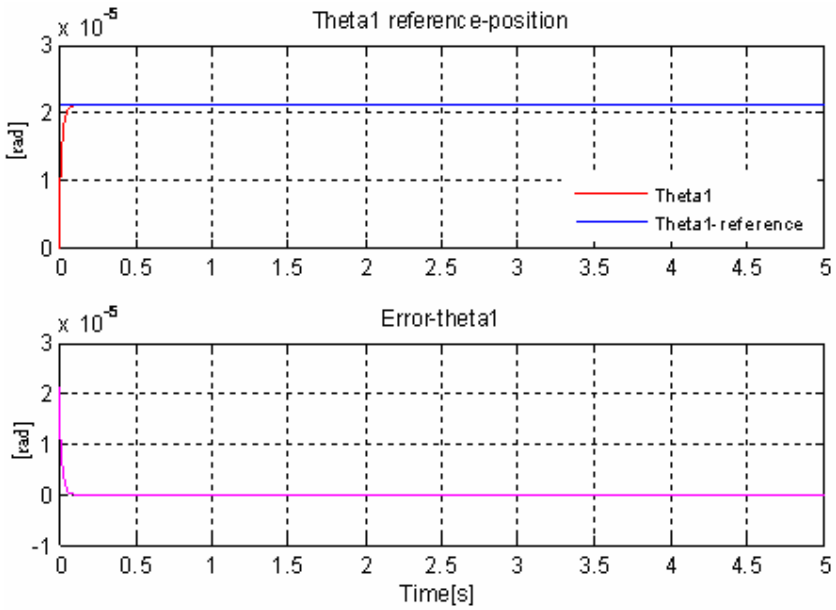

Figure 5-12 – System response for theta1

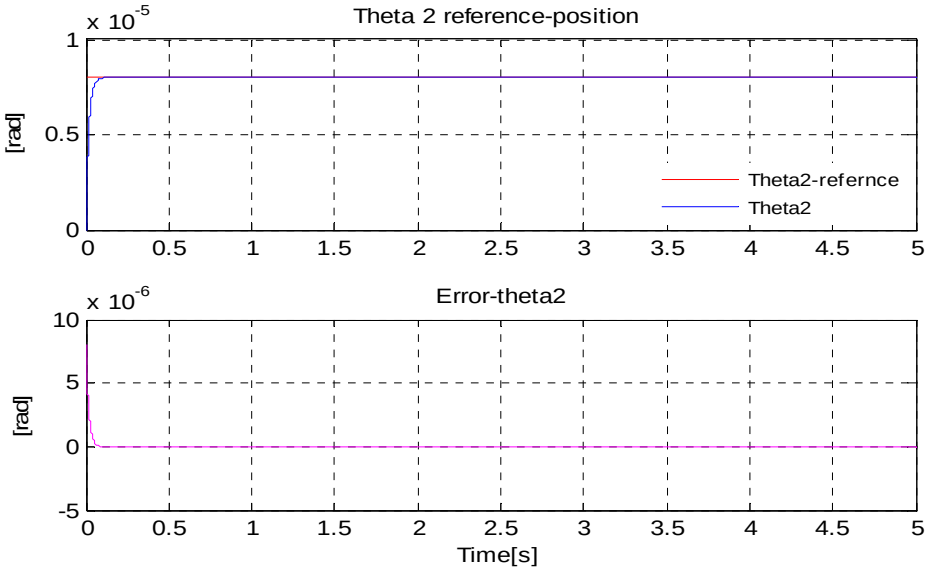

Figure 5-13 – System response for theta2

In this level, simulation results are satisfactory and positions reach their desired values fast than classical control.

Step _2: In one dimensional case, the number of functions and system freedom inequalities are solved using switching controller.

Controller can not control the motion at the same time for both x-y references so that trajectory tracking can be problematic. If P_4 wants to track a position including x and y references than control architecture has to be changed.

In order to solve the above problem some improvements should be done. One of the ways could be using jacobian or theta transformation if the system would be full actuated [18].

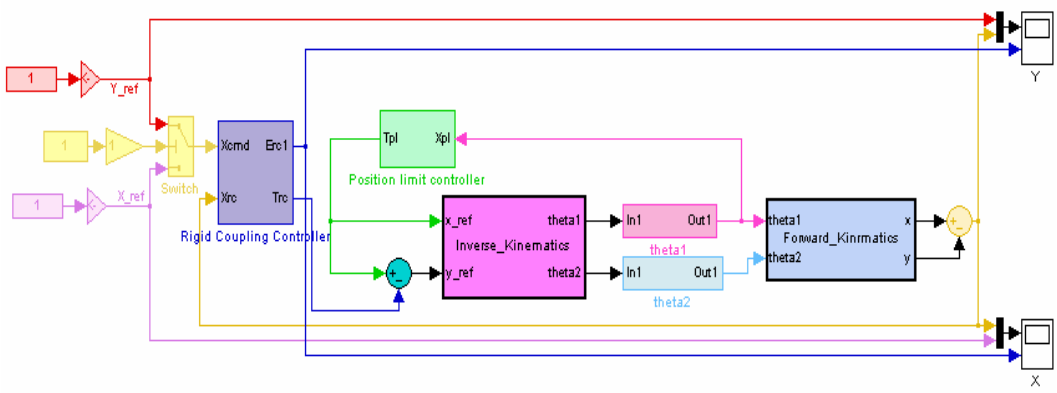

Figure 5-14 – Step_2 block diagram representation

Although logic and calculations are satisfactory in theory, it does not work in practice due to Matlab configuration parameters.

Step_3: The second method can be composed using classical control architecture and functional control architecture in the same framework. Figure 5-15 shows this combination.

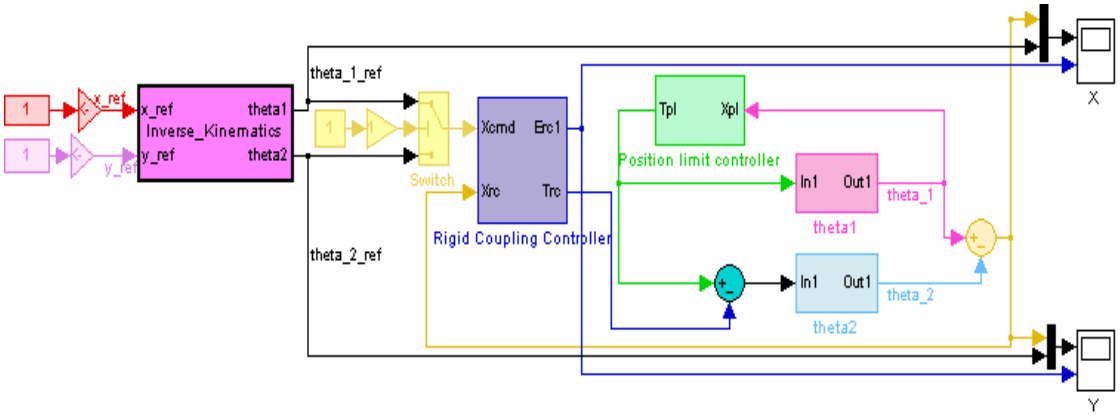

Figure 5-15 - Hybrid: Classical and functional control approach

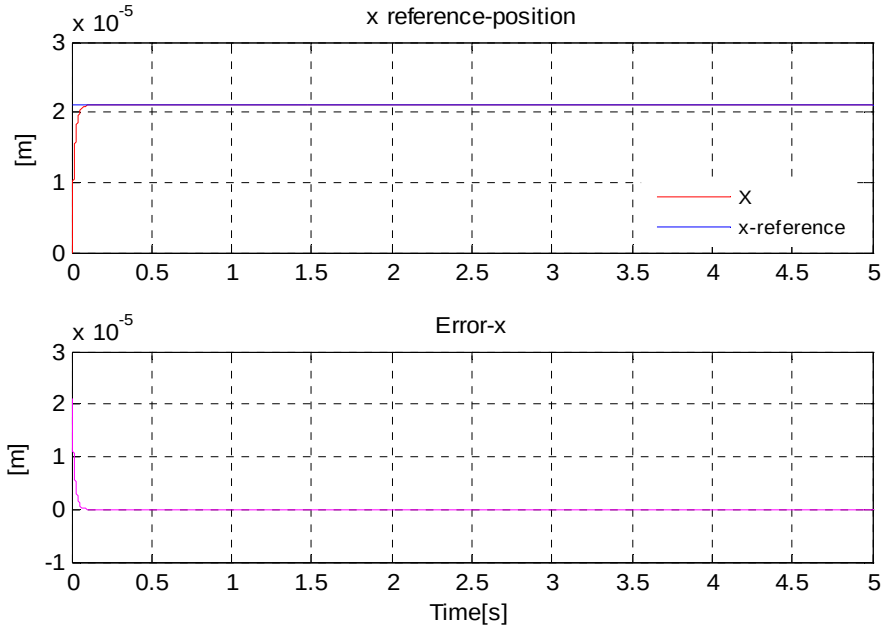

Figure 5-16 – Position response through x axis

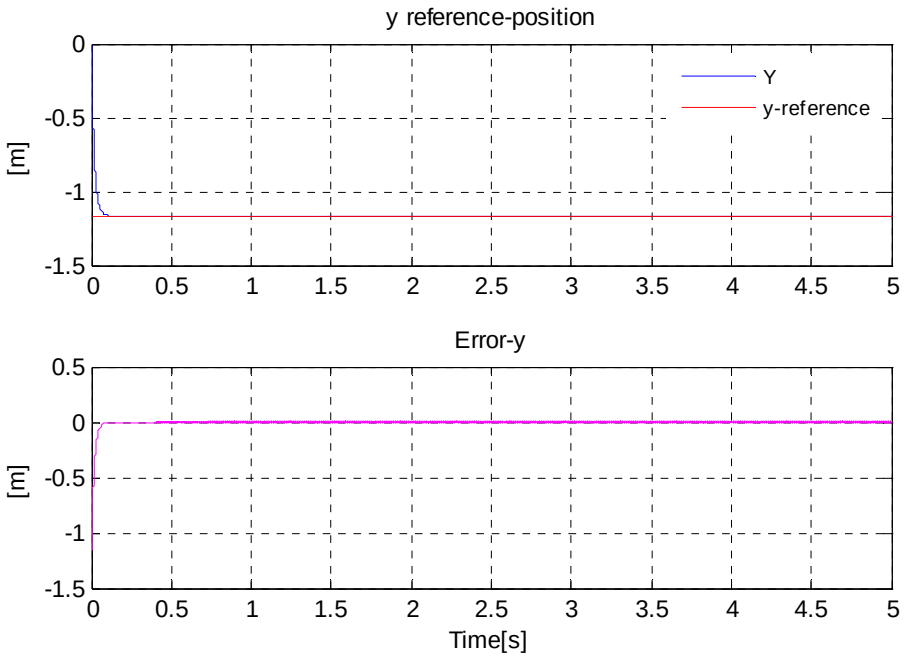

Figure 5-17 - Position response through y axis

This implementation works. The structure of system looks like classic control approach with function based controllers. Although it is satisfactory, motion can not be controlled as combination of x and y references. The future work will be developing this algorithm to trace a trajectory.

In this study decentralized controller is used to control the pantograph. It is a new point of view for parallel mechanisms. The classical control methods need computed torques which are based on dynamic equations. The simple and fast controller design is intended by using functional controller. The classic functions do not help to make the design easy. Instead of using those kinematic equations are investigated. Giving references as functions of trigonometric variables instead of θ_1, θ_2 is being developed.

If the classical controller is compared with functional controller and results are satisfactory. Although giving references at the same time for x and y direction is not possible for functional controller now, it will be developed.

5.6 Three-Legged Mechanism

In this part, the functional control approach will be demonstrated on the control of the Stewart Platform like parallel mechanism [35] in which the position and orientation of platform is defined by the length of the supporting linear actuators [37], [38], [39]. By enforcing certain relations among these actuators (for example if all are forced to maintain the same length the motion of the platform will be than in z axis only) the constrained motion of the system can be performed. By representing the task as a combination of these constrained motions in some cases the overall controller design becomes simpler and decoupling of the nonlinear dynamics can be achieved. In essence, the method is using Sliding Mode Control (SMC) design procedure [40], [41].

Simulation results are presented to compare the performance of observers on robot and function coordinates.

Figure 5-18 shows the systems is considered three dof. It consists of three serial links with prismatic joints and two triangular platforms; one of them is stable and the other one is moving. All distances between the legs are equal. The external torque can be given the center point of the moving platform.

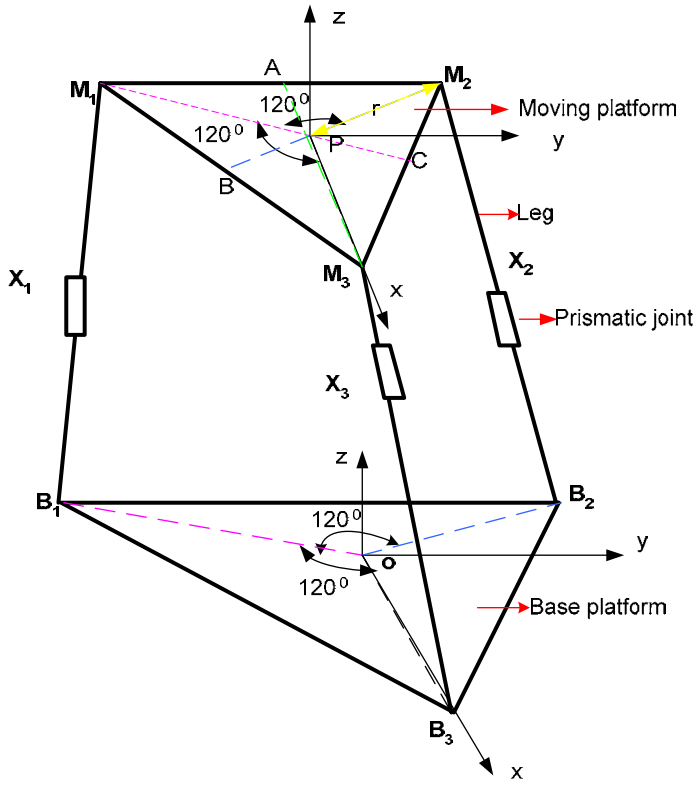

Figure 5-18 - General structure of three-legged robot

5.6.1 Function Based Control for Three-Legged Robot

Model of 3 dof parallel manipulator is shown in Figure 5-18. Each of the legs can be described by $m_i\ddot{x}_i + n_i\left(x_i, \dot{x}_i\right) = F_i - F_{disi} \quad i = 1,2,3$. Motion of the platform consists of the translational, which relates to the sum of the three legs positions and rotational motion with respect to some axis the simplest being defined by one leg length constant and the others varying in time so the rotation appears related to the difference in length of two legs. Based on this one can define the following functions to be controlled:

$$\varepsilon = x_1 + x_2 + x_3 \qquad \text{translation along z axis} \tag{71}$$

$$\varepsilon_{12} = x_1 - x_2 \qquad \text{rotation along } AM_3 \text{ axis} \tag{72}$$

$$\varepsilon_{13} = x_1 - x_3 \qquad \text{rotation along } BM_2 \text{ axis} \tag{73}$$

$$\varepsilon_{23} = x_2 - x_3 \qquad \text{rotation along } CM_1 \text{ axis} \tag{74}$$

The projection of the parallel mechanism motion on subspace defined by these functions may be easily obtained in the following form:

The common mode based for translational controller

The translational controller formulated depends on position of leg lengths along z-axis.

$$\ddot{\varepsilon} = \frac{1}{m_1}F_1 - \frac{F_{dis1}}{m_1} + \frac{1}{m_2}F_2 - \frac{F_{dis2}}{m_2} + \frac{1}{m_3}F_3 - \frac{F_{dis3}}{m_3} \tag{75}$$

$$u_i = \frac{F_i}{m_i}, i = 1,2,3, \; d_{123} = \sum_{i=1}^{3}\frac{F_{disi}}{m_i} \tag{76}$$

$$\ddot{\varepsilon} = u_1 + u_2 + u_3 - d_{123} \rightarrow \ddot{\varepsilon} = u_{123} - d_{123} \tag{77}$$

The dynamics on differential coordinates according to one of the rotating axis (AM_3, BM_2) are figured out as follows:

Rotation through the AM_3 axis:

$$\ddot{\varepsilon}_{12} = \frac{1}{m_1} F_1 - \frac{F_{dis1}}{m_1} - (\frac{1}{m_2} F_2 - \frac{F_{dis2}}{m_2}) \tag{78}$$

$$\ddot{\varepsilon}_{12} = u_1 - u_2 - d_{12} \rightarrow \ddot{\varepsilon}_{12} = u_{12} - d_{12} \tag{79}$$

Rotation through the BM_2 axis:

$$\ddot{\varepsilon}_{13} = \frac{1}{m_1} F_1 - \frac{F_{dis1}}{m_1} - (\frac{1}{m_2} F_3 - \frac{F_{dis3}}{m_3}) \tag{80}$$

$$\ddot{\varepsilon}_{13} = u_1 - u_3 - d_{13} \rightarrow \ddot{\varepsilon}_{13} = u_{13} - d_{13} \tag{81}$$

Following results presents transformation matrix; one should select such a set of functions so that transformation of control from functional space back to original space is unique. In our case we can select only three functions to be controlled at the same time. Assume we select $\varepsilon, \varepsilon_{12}, \varepsilon_{13}$ for which transformation matrix from original to function space can be written as in (82) and selected functions (or "virtual plants") are defined as in (77), (79), (81).

$$f_{Tl} = \begin{bmatrix} 1 & 1 & 1 \\ 1 & -1 & 0 \\ 1 & 0 & -1 \end{bmatrix} \tag{82}$$

Since all "virtual plants" are of the second order the controller should be designed in such a way that sliding mode is enforced on the intersection of the manifolds S_{ε_i} (i=1,2,3) :

$$S_{\varepsilon_i} = \left\{ (q, \dot{q}) : \ \xi_{\varepsilon_i}(\varepsilon_i, \dot{\varepsilon}_i) - \xi_{\varepsilon_i}^{ref}(\varepsilon_i, \dot{\varepsilon}_i) = \sigma_{\varepsilon_i} = 0 \right\} \tag{83}$$

Controllers that enforce sliding mode [41] and [42] on each of the surfaces are easy to determine as in (8). In order to look at different scenarios in designing the controllers we have developed two computer simulation models to check the dynamic formulation of three-legged parallel manipulator and compare the performance of disturbance observer on functional coordinate and on robot coordinates. Structures of the control systems are depicted in Figure 5-19 and Figure 5-22.

Parameters	Values
C	30
D	50
Ku	10^{-5}

Table 5-3 – Parameters used in Sliding mode controller

The actuator parameters used in simulation are taken from Table 5-3 with g =500 rad/s (cut off frequency of DOB), sampling time 0.1 ms.

5.6.2 Simulation results for Three-Legged Mechanism

System responses are shown DOB in robot space by Figure 5-20 & Figure 5-21 and in functional space by Figure 5-23 and Figure 5-24 for $2x10^{-6}$xsin(t) m reference with band-limited white noise (Amplitude: $2x10^{-6}$). As translational movement of common mode and rotational motions of difference mode of three legs positions are shown in the following figures.

5.6.2.1 Disturbance observer in robot space and simulation results

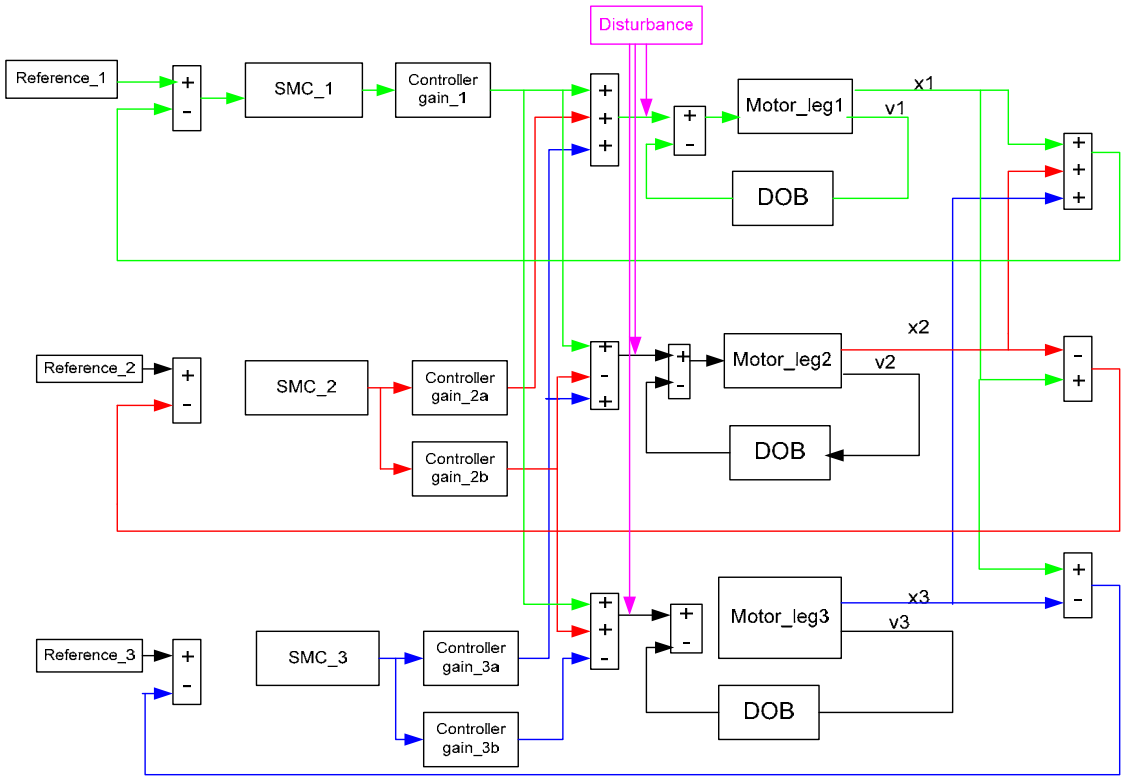

Figure 5-19 – Robot space bock diagram

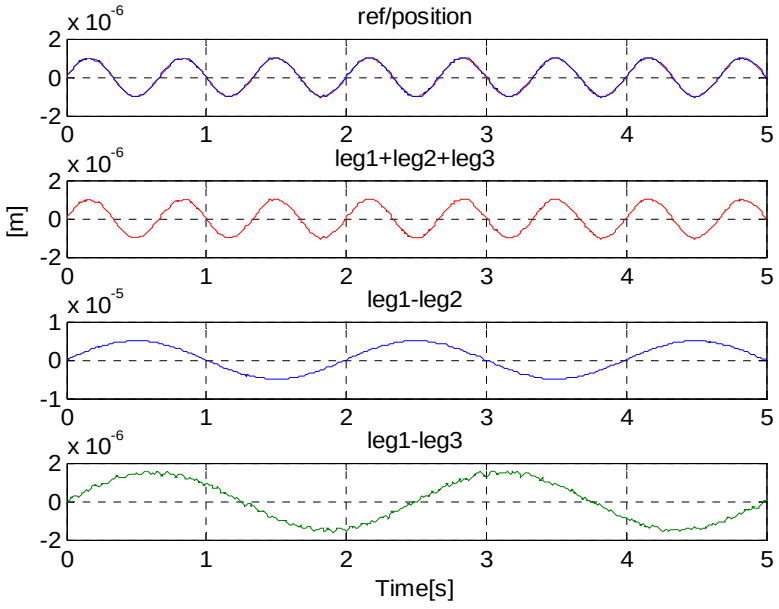

Figure 5-20 - Positions with disturbance

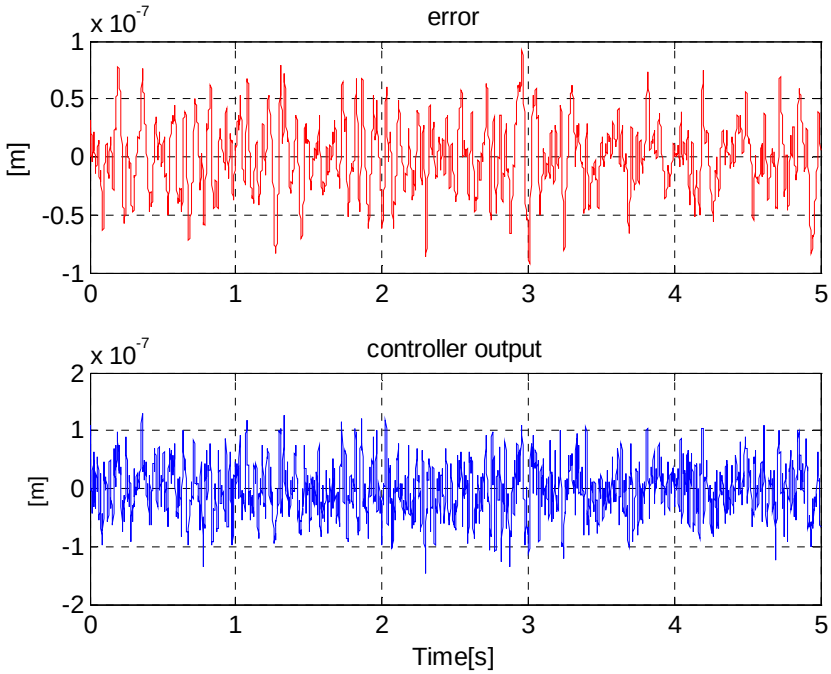

Figure 5-21 - Error and control output with disturbance

The simulation results show that functional controllers with disturbance observer on robot coordinate work well in order to realize system role.

5.6.2.2 Disturbance observer in function space and simulation results

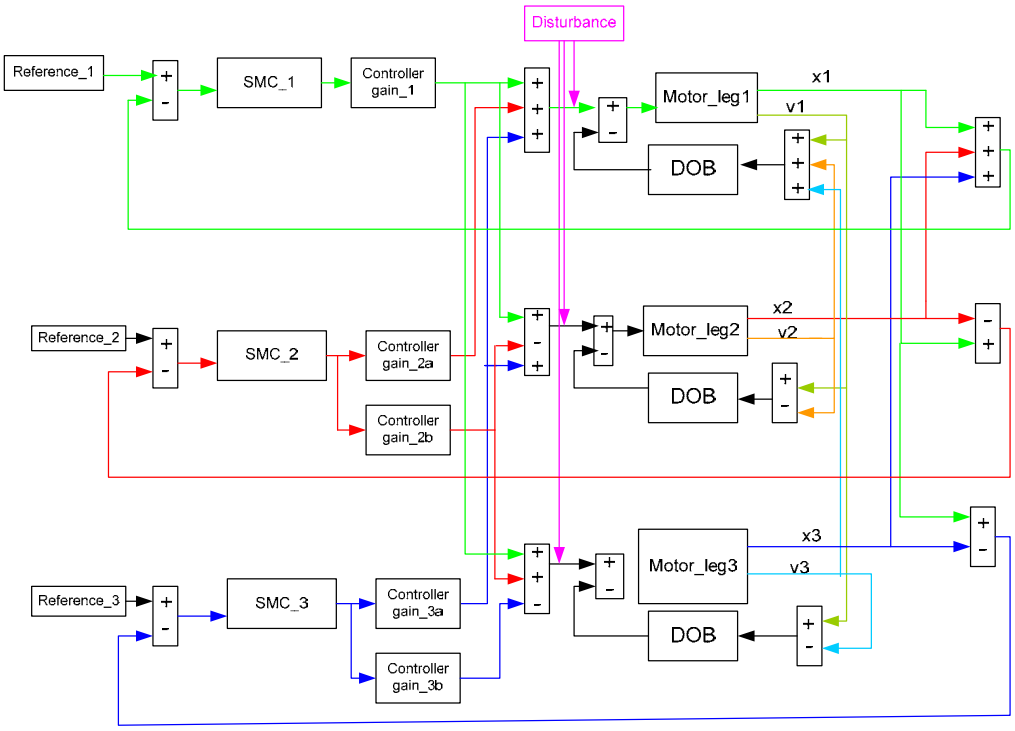

Figure 5-22 – Function space block diagram

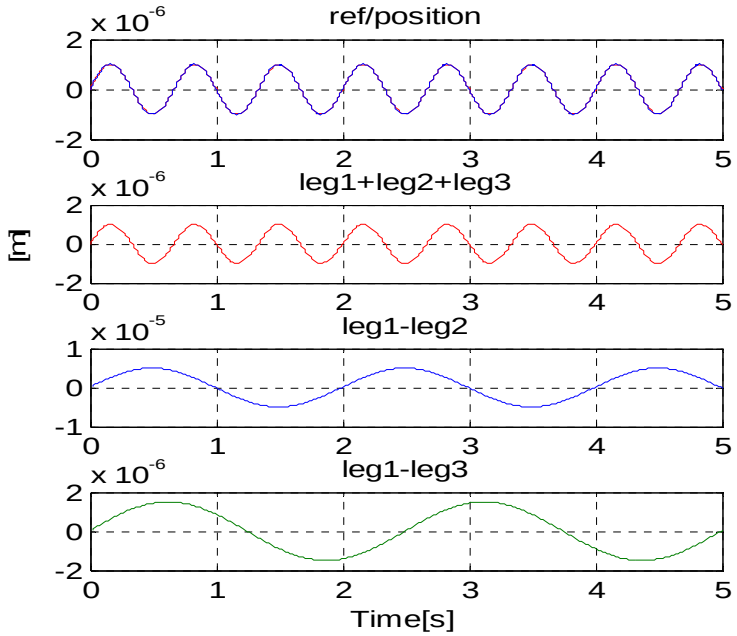

Figure 5-23 - Positions with disturbance

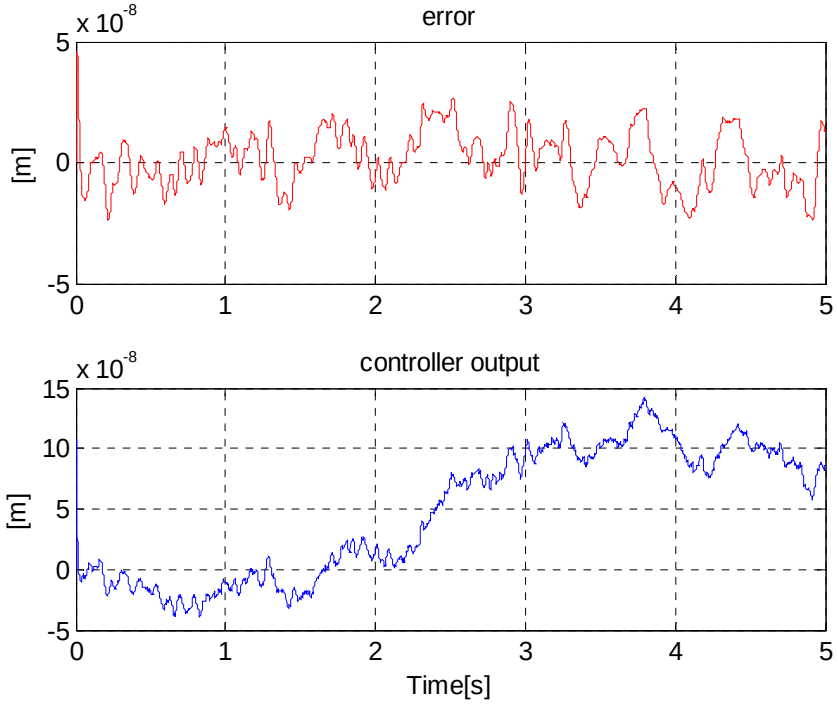

Figure 5-24 Error and control output with disturbance

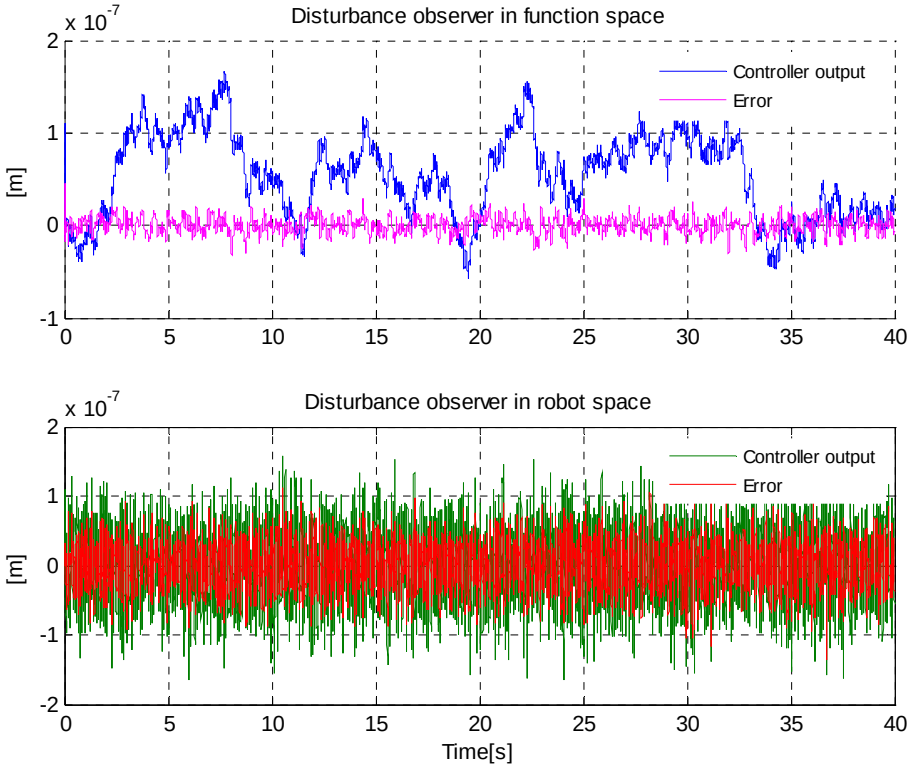

Figure 5-25- Errors and control outputs in robot and function spaces

The simulation results show that performance of functional controllers is satisfactory. When we have DOB in our functional space, controller performs better than robot space. Error amplitude and oscillations are less in function space.

In this study, a generalized approach to parallel manipulators is presented. It has been shown that due to system structure design can be performed so to guaranty the tracking in the "function space". The conditions for stability and integrity of such system design are found. As examples the manipulation of pantograph and three-legged parallel manipulators are presented.

6 CONCLUSION

In this work, we presented a generalized approach to motion control system and a possibility of projecting the system motion to a "functional space" in which natural tasks of the system are presented. Concerned motion systems are the systems which should maintain its trajectory despite of interaction with other systems, or which should modify its behavior in order to maintain virtual or real specified interactions.

In order to show the feasibility of functionality two active fields of research are blended: the field of bilateral control and the subject of parallel manipulators. Satisfactory simulation results encouraged that modern motion control systems can fulfill the complicated system requirements with simple controllers via functional controller design.

It has been shown that motion control tasks can be formulated as a requirement to enforce stability in selected manifold in state space of the system. The approach is applicable for systems with and without contact with environment that leads to unified formulation of the control tasks.

7 REFERENCES

[1] R. A. Brooks, "A Robust Layered Control System For A Mobile Robot", *IEEE J. R & A*, vol. RA-2, No. 1, pp. 14–23, 1986.

[2] M. Cossentino, L Sabatucci and A. Chella, "A Possible Approach to the Development of Robotic Multi-Agent Systems", *Proc. IEEE/WIC Int.Conf.Intelligent Agent Technology*, pp. 539–544, 2003.

[3] T. Ueyama, T. Fukuda, F. Arai, Y. Katou, S. Matsumura and T. Uesugi "A Study on Dynamically Reconfigurable Robotic Systems", *J. JSME*, (10th Report, Distributed Control Structure for Organization using an Evaluation of Network Energy for Group Structure of Cebot), Part C, Vol. 58, No. 549, pp. 132–139, (in Japanese), 1992.

[4] Y. Fujimoto, T. Sekiguchi, "Fault-Tolerant Configuration of Distributed Discrete Controllers", *IEEE Trans. on Industrial Electronics*, vol. 50, No. 1, pp. 86–93, 2003.

[5] J. E Hernandez, A. G. Loukianov, B. Castillo-Toledo, V. I. Utkin, "Observer Based Decomposition Control of Linear Delayed Systems", *Proc. IEEE Int. Conf. Decision and Control*, pp. 1867–1872, 2001.

[6] S. Arimoto, P. T. A Nguyen, "Principle of Superposition for Realizing Dexterous Pinching Motions of a Pair of Robot Fingers with Soft-tips", *IEICE Trans. Fundamentals*, vol. E84-A, No. 1, pp. 39–47, 2001.

[7] M. Okada, K. Tatani, Y. Nakamura, "Polynomial Design of the Nonlinear Dynamics for the Brain-Like Information Processing of Whole Body Motion", *Proc. of IEEE Int. Conf. on R & A*, pp. 1410–1415, 2002.

[8] T. Tsuji, K. Ohnishi, "A Controller Design Method of Decentralized Control System", *IEEJ Int. Power Electronics Conf.*, IPEC-NIIGATA, 2005.

[9] Onal, C. D. and A. Sabanovic (2005). Bilateral Control with a Reflex Mechanism on the Slave Side, Proc. of the *31st Annual Conf. of the IEEE Industrial Electronics Society (IECON2005)*, pp. 195–200.

[10] D.A Lawrance, "Stability and Transparency in Bilateral Teleoperation", *IEEE Trans. R & A*, Vol. 9, No. 5, pp.624-637,1993,

[11] D. A. Lawrence, "Stability and Transparency in Bilateral Teleoperation", *Proceeding of the 31st Conference on Decision and Control*, Tucson, Arizona, December 1992.

[12] K. H. Zaad and S. E. Salcudean, "On the Use of Local Force Feedback for Transparent Teleoperation", *Proceedings of IEEE International Conference on Robotics and Automation*, Detroil, Michigan, May 1999.

[13] S. Katsura, "Advanced Motion Control Based on Quarry of Environmental Information", *Phd Report*, Keio University, Japan.

[14] Y. Yokokohji, N. Hosotani, T. Yoshikawa, "Analysis of Maneuverability an Stability of Micro-Teleoperation Systems", *IEEE*, 1050-4729/94 $03.33 © 1994.

[15] Y.Yokokohhji and T. Yoshikawa, "Bilateral Control of Master-Slave Manipulators for Ideal Kinesthetic Coupling", *Proc. IEEE Conf. R & A*, pp.849-858, 1992.

[16] M. Elitaş, A. Şabanoviç, "Controlling Interactions in Motion Control Systems", *The 5th IFAC Intl. WS DECOM-TT 2007*, May 17-20, Cesme, Turkey.

[17] A. Şabanoviç, M. Elitaş, "SMC Based Bilateral Control", *2007 IEEE International Symposium on Industrial Electronics*, June 4-7, Caixanova-Vigo, Spain.

[18] T. Tsuji, "Motion Control for Adaptation to Human Environment", *PhD Report*, 2005.

[19] M. Elitaş, E. Deniz, M. Acer, Asıf Şabanoviç, "Functional Control for Bilateral Systems" (in Turkish), *TOK'06,* Ankara, Turkey.

[20] G. D. Gersem, "Kinaesthetic Feedback and Enhanced Sensitivity in Robotic Endoscopic Telesurgery", *PhD Report*, Katholieke Universiteit Leuven, Belgium.

[21] S. Katsura, Y. Matsumoto, and K. Ohnishi, "Modeling of Force Sensing and Validation of Disturbance Observer for Force Control", 0-7803-7906-3/03/$17.00 ©2003 IEEE.

[22] A. Altınışık: "Bilateral Control – Operational Enhancements" *MSc Report*, Sabanci University, 2006.

[23] P. F. Hokayem, M. W. spong, "Bilateral Teleoperation: An Historical Survey", *Preprint submitted to Automatica*, 15 February 2005.

[24] http://en.wikipedia.org/wiki/Haptics, 20 June 2007

[25] T. Tsuji, K. Ohnishi, "Controller Design Method Based on Functionality",

[26] K. Ohnishi, M. Shibata, T. Murakimi, "Motion control for Advance Mechatronics", *Transaction on Mechatronics*, IEEE, Vol. 1, No. 1, pp. 56-67

[27] S. Katsura, W. Lida, K. ohnishi, "Medical Mechatronics – An Application to Haptic Forceps", *Annual Reviews in Control*, Elsevier, 13 May 2005.

[28] D. J. Abbott, C. Becke, R. I. Rothstein, and W. J. Peine, "Design of an Endoluminal NOTES Robot Systems", Preprint submitted to *2007 IEEE/RSJ International Conference on Intelligent Robots and Systems*. Recived April 9, 2007.

[29] L. Barbe, B. Bayle, and M. de Mathelin, "Bilateral Controllers for Teleoperated Percutaneous Intervantions: Evaluation and Improvements", *Proceedings of the 2006 American Control Conference Minneapolis,* Minnesota, USA, June 14-16, 2006.

[30] N. Simaan, "Analysis and Synthesis of Parallel Robots for Medical Applications", *The Degree of Master Science in Mechanical Engineering*, Israel Institute of Technology , July 99.

[31] J. P. Merlet, "Parallel Robots", Second Edition, INIRIA, Sophia-Antipolis, France, 2006 Spinger.

[32] H. Yu, "Modeling and Control of Hybrid Machine Systems – five-bar Mechanism Case", *International Journal of Automation and Computing*, 235-243 2006.

[33] G. Camion, Q. Wang, V. Hayward, "The pantograph Mk-II: A Haptic Instrument", *IEEE/RSJ International Conference on Intelligent Robots an Systems*, 2005.

[34] T. Tsuji, K. Ohnishi, A. Sabanovic, "A Controller Design Method Based on Functionality", AMC 2006, Istanbul, Turkey.

[35] E. F. Fichter, "A Stewart Platform-Based Manipulator: General Theory And Practical Construction", *Int. J. Robotics Res*., vol. 5, no. 2, Summer 1986.

[36] T. Tsuji, K Natori, K. Ohnishi, "A Controller Design Method of Bilateral Control System," *EPE-PEMC'04*, Vol. 4, pp. 123–128, 2004.

[37] K. Lee and D. K. Shah, "Kinematic Analysis of A Three Degrees of Freedom in-Parallel Actuated Manipulators", *in Proc. IEEE Int. Conf. Robotics and Automation*, vol.1 Raleigh, NC, Mar. 31-Apr. 3 1987, pp.345-350.

[38] R. Di Gregoria and V. Parenti-Castelli, "A Translational 3-DOF Parallel Manipulator", *in Recent Advances in Robot Kinematics: Analysis and Control*

(Lenaric J., Husty M. L. Eds.), Klıwer, pages 401-410,1998.

[39] Y. Li and Q. Xu, "Kinematics and Dexterity Analysis for A Novel 3 Dof Translational Manipulator", *Proceedings of the 2005 IEEE International Conference on Robot & Automation*, Barcelona, Spain, April 2005

[40] A. Şabanoviç, K. Abidi, M. Elitaş, "A Study on High Accuracy Discrete-time Sliding Mode Control, *12th International Power Electronics and Motion Control Conference EPE- PEMC 2006,* Portoroz, Slovenia, August 30-September 1, 2006.

[41] A. Şabanoviç, "Sliding Modes in Power Electronics and Motion Control Systems", *Proceedings of the 29th IEEE Annual Conference of the IEEE Industrial Electronics Society* IECON '03-ROANOKE, pp. 997–1002, 2003.

[42] A. Şabanoviç, S. Khan, M. Elitaş, K. Jezernik "Sliding Mode Adaptive Controller for PZT Actuators", *32nd Annual Conference of the IEEE Industrial Electronics Society*, Paris, November 7-10, 2006.

[43] E. Deniz, M. Elitaş, Asıf Şabanoviç, ″Design of Haptic Devices for Micro Parts Handling ″ (in Turkish), *TOK'06*, Ankara, Turkey.

[44] S. Katsura, Y. Matsumoto, and K. Ohnishi,"Analysis and Experimental Validation of Force Bandwith for Force Control", IEEE Transactions on Industrial Electronics, Vol. 53, NO.3, June 2006.

[45] E. Deniz, "Design of Haptic Device for Micro Parts Handling", *MSc Report,* University of Twente, 2005.